MIMO Energy Harvesting in Full-Duplex Multi-User Networks

Tam, H. H. M., Tuan, H. D., Nasir, A. A., Duong, Q., & Poor, H. V. (2017). MIMO Energy Harvesting in Full-Duplex Multi-User Networks. *IEEE Transactions on Wireless Communications*, *16*(5), 3282-3297. https://doi.org/10.1109/TWC.2017.2679055

Published in:
IEEE Transactions on Wireless Communications

Document Version:
Peer reviewed version

MIMO Energy Harvesting in Full-Duplex Multi-user Networks

H. H. M. Tam, H. D. Tuan, A. A. Nasir, T. Q. Duong and H. V. Poor

***Abstract*—The paper aims at the efficient design of precoding matrices for the sum throughput maximization under throughput QoS constraints and energy harvesting (EH) constraints for energy-constrained devices in a full-duplex (FD) multicell multi-user multiple-input-multiple-output (MU-MIMO) network. Both time splitting (TS) and power splitting (PS) are considered to ensure practical EH and information decoding (ID). These problems are quite complex due to highly non-concave objectives and nonconvex constraints. Especially, with TS, which is implementation-wise quite simple, the problem is even more challenging because time splitting variable is not only coupled with the downlink (DL) throughput function but also coupled with the self-interference (SI) in the uplink (UL) throughput function. New path-following algorithms are developed for their solutions, which just require a single convex quadratic program for each iteration and ensure fast convergence too. Finally, the FD EH maximization problem under throughput QoS constraints in TS is also considered. The performance of the proposed algorithms is also compared with that of the modified problems assuming half-duplex systems. In the end, the merit of the proposed algorithms is shown through extensive simulations.**

***Index Terms*—Full-duplexing transceiver, energy harvesting, information precoder, energy precoder, path-following algorithm, matrix inequality**

I. Introduction

Recently, wireless energy harvesting (i.e. energy constrained devices scavenge energy from the surrounding RF signals) is gaining more and more attraction from both industry and academia [1], [2]. Since the amount of energy opportunistically harvested from the ambient/natural energy sources is uncertain and cannot be controlled, base stations (BSs) in small-cell networks can be configured to become dedicated and reliable wireless energy sources [3]. The small cell size not only gives the benefit of efficient resource reuse across a geographic area [4] but also provides an adequate amount of RF energy to battery powered user equipments (UEs) for practical applications [1], [2], [5] due to the close BS-UE proximity. In order to transfer both energy and information by the same communication channel, UEs are equipped with both information decoding receiver and energy harvesting receiver. Since the received signal cannot be used for energy harvesting after being decoded, there are two available implementations for wireless energy harvesting and information decoding: (i) receive power splitting in which a receiver splits the received signal into two streams of different power for decoding information and harvesting energy separately and (ii) transmit time splitting to enable the receiver to decode information for a portion of a time frame and harvest energy for the rest. Beamforming can be applied to focus the RF signal to energy harvesting receiver or enhance throughput at information decoding receiver [5].

Most of the previous works (see e.g. [6], [7] and references therein) only focus on beamforming power optimization subject to ID throughput and EH constraints with PS in multi-input single-output (MISO) networks. The ID throughput constraints are equivalent to signal-to-interference-plus-noise ratio (SINR) constraints, which are indefinite quadratic in beamforming vectors. The harvested energy constraints are also indefinite quadratic constraints. Thus, [6], [7] used semi-definite relaxation (SDR) to relax such indefinite quadratic optimization problems to semi-definite programs (SDP) by dropping the matrix rank-one constraints on the outer products of beamforming vectors. The variable dimension of SDP is explosively large, and the beamforming vectors that are recovered based on the matrix solution of SDR perform poorly [8]. Moreover, SDR cannot be applied to throughput or EH maximization as the problems resultant by SDR are still highly nonconvex. Only recently there was an effective development to address these problems in [9] and [10].

Considering multi-input multi-output (MIMO) interference channels, information throughput and harvested energy, i.e., rate-energy (R-E) trade-off, was investigated in [11] and [12], assuming that any UE either acts as an ID receiver or an EH receiver. In case that UEs can operate both as an ID receiver and EH receiver (namely co-located cases), the R-E region of point-to-point MIMO channel was studied in [13]. Note that in MIMO networks, the information throughput function is involved with the determinant operation of a matrix and can no longer be expressed in the form of SINR. Consequently, the throughput constraints are always very challenging in precoding signals. [14], [15] used zero-forcing or interference-alignment to cancel all interferences, making the throughput functions concave in the signal covariance. The covariance optimization becomes convex but it is still computationally

This work was supported in part by the Australian Research Councils Discovery Projects under Project DP130104617, in part by the U.K. Royal Academy of Engineering Research Fellowship under Grant RF1415/14/22 and U.K. Engineering and Physical Sciences Research Council under Grant EP/P019374/1, and in part by the U.S. National Science Foundation under Grants CNS-1456793 and ECCS-1647198.

Ho Huu Minh Tam and Hoang Duong Tuan are with the Faculty of Engineering and Information Technology, University of Technology Sydney, Broadway, NSW 2007, Australia (email: huuminhtam.ho@student.uts.edu.au, Tuan.Hoang@uts.edu.au).

Ali Arshad Nasir is with the Department of Electrical Engineering, King Fahd University of Petroleum and Minerals (KFUPM), Dhahran, 31261, KSA (Email: anasir@kfupm.edu.sa).

Trung Quang Duong is with Queen's University Belfast, Belfast BT7 1NN, U.K. (Email: trung.q.duong@qub.ac.uk)

H. Vincent Poor is with the Department of Electrical Engineering, Princeton University, Princeton, NJ 08544 USA (e-mail: poor@princeton.edu).

difficult with no available algorithm of polynomial time. Moreover, there is no known method to recover the precoder matrices from the signal covariance. Only recently, the MIMO throughput function optimization has been successfully addressed for non-EH system in our previous work via a successive convex quadratic programming [16]. The result of [16] can be adapted to MIMO networks that employ EH by PS approach. However, there is almost no serious research for the systems employing TS in MIMO networks. Though TS-based system is practically easier to implement, the related formulated problem is quite complex because the throughput function in such case is coupled with the TS variable that defines the portion of time slot dedicated to EH and ID. This renders the aforementioned precoder design [14]–[16] for PS inapplicable. To the best of our knowledge, both the throughput maximization problem and the harvested energy maximization problem with TS are still very open.

All aforementioned works only assume that UEs only harvest energy arriving from BSs' downlink (DL) transmission. In reality, UEs can also opportunistically harvest energy from other UEs' signals during their uplink (UL) transmission. Furthermore, by allowing the BSs to simultaneously transmit and receive information, both the spectral efficiency and the amount of transferred energy will be improved. With the recent advances in antenna design and RF circuits in reducing self-interference (SI) [17]–[20], which is the interference from a BS's DL transmission to its UL receiver, the full duplex (FD) technology is recently proposed as one of the key transceiving techniques for the fifth generation (5G) networks [20]–[24]. In this paper, we are interested in a network in which each FD multi-antenna BS simultaneously serves a group of UL UEs (ULUs) and a group of DL UEs (DLUs). In the same time, the BS also transfers energy to DLUs via TS or PS. FD transmission introduces even more interferences into the network by adding not only SI but also the interference from UL users (ULUs) toward downlink users (DLUs) and the interference from DL transmission of other BSs. Consequently, the UL and DL precoders are coupled in both DL and UL throughput functions, respectively, which makes the optimization problems for UL transmission and DL transmission inseparable.

In literature, [14], [25], [26] proposed covariance matrices design in (non-EH) FD MU-MIMO networks using D.C. iterations [27], which are still very computationally demanding as they require log-determinant function optimizations as mentioned above. Our previous work [16] has recently proposed a framework to directly find the optimal precoding matrices for the sum throughput maximization under throughput constraints in FD MU-MIMO multi-cell networks, which requires only a convex quadratic program of moderate size in each iteration and thus is very computationally efficient.

In this paper, we propose the design of efficient precoding matrices for the network sum throughput maximization under QoS in terms of MIMO throughput constraints and EH constraints in an FD EH-enabled multicell MU-MIMO network. Both PS and TS are considered for the precoder designs and called by PS problem and TS problem, respectively. They are quite challenging computationally due to nonconcave objective function and nonconvex constraints. However, we will see that the PS problem can be efficiently addressed by adapting the algorithm of [16]. On the other hand, the TS problem is much more challenging because the TS variable $\boldsymbol{\alpha}$ is not only coupled with the DL throughput function but also coupled with the SI in the UL throughput function. It is nontrivial to extend [16] to solve the problem for the TS problem. Toward this end, we develop a new inner approximation of the original problem and solve the problem by a path-following algorithm. Finally, we also consider the FD EH maximization problem with throughput QoS constraints with TS. This problem also has a nonconvex objective function and nonconvex constraints and will be addressed by applying an approach similar to that of proposed for the TS problem.

The rest of this paper is organized as follows: Section II presents the system model the SCP algorithm of the PS problem. The main contribution of the paper is Section III and Section IV, which develop algorithms for the TS problem and FD EH maximization problem. Section V evaluates the performance of our devised solutions by numerical examples. Finally, Section VI concludes the paper.

Notation. All variables are boldfaced. I_n denotes the identity matrix of size $n\times n$. The notation $(.)^H$ stands for the Hermitian transpose. $|A|$ denotes the determinant of a square matrix A and $\langle A\rangle$ denotes the trace of a matrix A. $(A)^2$ is Hermitian symmetric positive definite AA^H. The inner product $\langle X, Y\rangle$ is defined as $\langle X^H Y\rangle$ and therefore the Frobenius squared norm of a matrix X is $||X||^2 = \langle (X)^2\rangle$. The notation $A \succeq B$ ($A \succ B$, respectively) means that $A - B$ is a positive semidefinite (definite, respectively) matrix. $\mathbb{E}[.]$ denotes the expectation operator and $\Re\{.\}$ denotes the real part of a complex number.

The following concept of function approximation [28] plays an important in our development.

Definition. A function $\tilde{f}$ is called a (global) minorant of a function f at a point $\bar{x}$ in the definition domain $\text{dom}(f)$ of f if $\tilde{f}(\bar{x}) = f(\bar{x})$ and $f(\mathbf{x}) \geq \tilde{f}(\mathbf{x})\ \forall\ \mathbf{x} \in \text{dom}(f)$.

The following result [16] is used.

Theorem 1: For function $f(\mathbf{V}, \mathbf{Y}) = \ln|I_n + \mathbf{V}^H\mathbf{Y}^{-1}\mathbf{V}|$ in matrix variable $\mathbf{V} \in \mathbb{C}^{n\times m}$ and positive definite matrix variable $\mathbf{Y} \in \mathbb{C}^{m\times m}$, the following quadratic function is its minorant at $(\bar{V}, \bar{Y})$

$$\tilde{f}(\mathbf{V}, \mathbf{Y}) = a + 2\Re\{\langle \mathcal{A}, \mathbf{V}\rangle\} - \langle \mathcal{B}, \mathbf{V}\mathbf{V}^H + \mathbf{Y}\rangle,$$

where $0 > a \triangleq f(\bar{V}, \bar{Y}) - \langle \bar{V}^H\bar{Y}^{-1}\bar{V}\rangle$, $\mathcal{A} = \bar{Y}^{-1}\bar{V}$ and $0 \preceq \mathcal{B} = \bar{Y}^{-1} - (\bar{Y} + \bar{V}\bar{V}^H)^{-1}$.

II. EH-enabled FD MU-MIMO Networks

We consider an MU-MIMO EH-enable network consisting of I cells. In cell $i \in \{1, \ldots, I\}$, a group of D DLUs in the downlink (DL) channel and a group of U ULUs in uplink (UL) channel are served by a BS i as illustrated in Fig. 1. Each BS operates in the FD mode and is equipped with $N \triangleq N_1 + N_2$ antennas, where N_1 antennas are used to transmit and the remaining N_2 antennas to receive signals. In cell i, DLU (i, j_{D}) and ULU (i, j_{U}) operate in the HD mode and each is equipped with N_r antennas. In the DL,

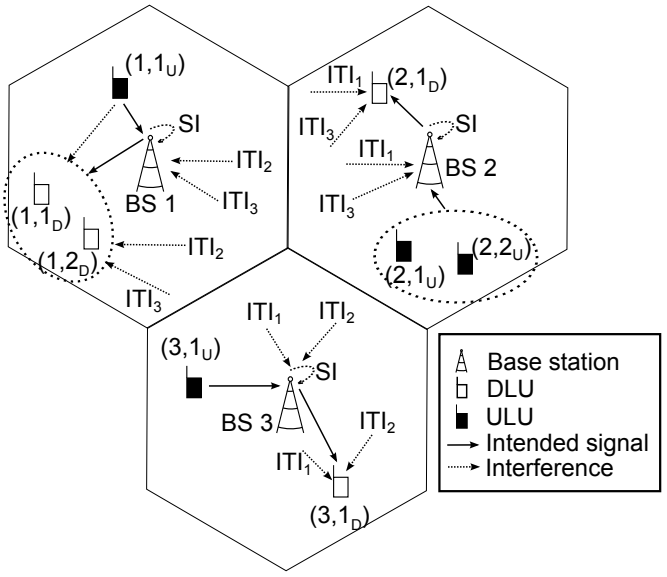

Fig. 1. Interference scenario in an FD multicell network, where SI denotes the self-interference and ITI_i denotes the interference from the BS and ULUs of cell i.

let $s_{i,j_\mathsf{D}} \in \mathbb{C}^{d_1}$ be the symbol intended for DLU (i, j_D) where $\mathbb{E}\left[s_{i,j_\mathsf{D}}(s_{i,j_\mathsf{D}})^H\right] = I_{d_1}$, d_1 is the number of concurrent data streams and $d_1 \leq \min\{N_1, N_r\}$. The vector of symbols s_{i,j_D} is precoded and transmitted to DLU (i, j_D) through the precoding matrix $\mathbf{V}_{i,j_\mathsf{D}} \in \mathbb{C}^{N_1 \times d_1}$. Analogously, in the UL, $s_{i,j_\mathsf{U}} \in \mathbb{C}^{d_2}$ is the information symbols sent by ULU (i, j_U) and is precoded by the precoding matrix $\mathbf{V}_{i,j_\mathsf{U}} \in \mathbb{C}^{N_r \times d_2}$, where $\mathbb{E}\left[s_{i,j_\mathsf{U}}(s_{i,j_\mathsf{U}})^H\right] = I_{d_2}$, d_2 is the number of concurrent data streams and $d_2 \leq \min\{N_2, N_r\}$. For notational convenience, let us define

$$\begin{gathered}\mathcal{I} \triangleq \{1, 2, \ldots, I\}; \quad \mathcal{D} \triangleq \{1_\mathsf{D}, 2_\mathsf{D}, \ldots, D_\mathsf{D}\};\\ \mathcal{U} \triangleq \{1_\mathsf{U}, 2_\mathsf{U}, \ldots, U_\mathsf{U}\}; \mathcal{S}_1 \triangleq \mathcal{I} \times \mathcal{D}; \quad \mathcal{S}_2 \triangleq \mathcal{I} \times \mathcal{U};\\ \mathbf{V}_\mathsf{D} = [\mathbf{V}_{i,j_\mathsf{D}}]_{(i,j_\mathsf{D})\in\mathcal{S}_1}; \mathbf{V}_\mathsf{U} = [\mathbf{V}_{i,j_\mathsf{U}}]_{(i,j_\mathsf{U})\in\mathcal{S}_2};\\ \mathbf{V} \triangleq [\mathbf{V}_\mathsf{D}\ \mathbf{V}_\mathsf{U}];\end{gathered}$$

In the DL channel, the received signal at DLU (i, j_D) is expressed as:

$$\begin{aligned} y_{i,j_\mathsf{D}} \triangleq & \underbrace{H_{i,i,j_\mathsf{D}}\mathbf{V}_{i,j_\mathsf{D}}s_{i,j_\mathsf{D}}}_{\text{desired signal}} \\ & + \underbrace{\sum_{(m,\ell_\mathsf{D})\in\mathcal{S}_1\setminus(i,j_\mathsf{D})} H_{m,i,j_\mathsf{D}}\mathbf{V}_{m,\ell_\mathsf{D}}s_{m,\ell_\mathsf{D}}}_{\text{DL interference}} \\ & + \underbrace{\sum_{\ell_\mathsf{U}\in\mathcal{U}} H_{i,j_\mathsf{D},\ell_\mathsf{U}}\mathbf{V}_{i,\ell_\mathsf{U}}s_{i,\ell_\mathsf{U}}}_{\text{UL intracell interference}} + n_{i,j_\mathsf{D}}, \end{aligned} \tag{1}$$

where $H_{m,i,j_\mathsf{D}} \in \mathbb{C}^{N_r \times N_1}$ and $H_{i,j_\mathsf{D},\ell_\mathsf{U}} \in \mathbb{C}^{N_r \times N_r}$ are the channel matrices from BS m to DLU (i, j_D) and from ULU (i, ℓ_U) to DLU (i, j_D), respectively. Also, n_{i,j_D} is the additive white circularly symmetric complex Gaussian noise with variance σ_D^2. In this work, the UL intercell interference is neglected since it is very small compared to the DL intercell interference due to the much smaller transmit power of ULUs. Nevertheless, it can be incorporated easily in our formulation.

Assuming that DLUs are equipped by both devices for ID and EH, the power splitting technique is applied at each DLU to simultaneously conduct information decoding and energy harvesting. The power splitter divides the received signal y_{i,j_D} into two parts in the proportion of $\boldsymbol{\alpha}_{i,j_\mathsf{D}} : (1 - \boldsymbol{\alpha}_{i,j_\mathsf{D}})$ where $\boldsymbol{\alpha}_{i,j_\mathsf{D}} \in (0, 1)$ is termed as the PS ratio for DLU (i, j_D). In particular, the signal split to the ID receiver of DLU (i, j_D) is given by

$$\sqrt{\boldsymbol{\alpha}_{i,j_\mathsf{D}}}y_{i,j_\mathsf{D}} + z^c_{i,j_\mathsf{D}}, \tag{2}$$

where each r-th element of z^c_{i,j_D} (i.e. $|z^c_{i,j_\mathsf{D},r}|^2 = \sigma_c^2$, $r = 1, .., N_r$) is additional noise introduced by the ID receiver circuity. An EH receiver processes the second part of the split signal $\sqrt{1 - \boldsymbol{\alpha}_{i,j_\mathsf{D}}}y_{i,j_\mathsf{D}}$ for the harvested energy

$$\sqrt{\zeta_{i,j_\mathsf{D}}(1 - \boldsymbol{\alpha}_{i,j_\mathsf{D}})}y_{i,j_\mathsf{D}},$$

where $\zeta_{i,j_\mathsf{D}} \in (0.4, 0.6)$ is the efficiency of energy conversion.

It follows from the receive equation (1) and the split equation (2) that the downlink information throughput at DLU (i, j_D) is

$$\begin{aligned} & f_{i,j_\mathsf{D}}(\mathbf{V}_\mathsf{D}, \mathbf{V}_\mathsf{U}, \boldsymbol{\alpha}_{i,j_\mathsf{D}}) \triangleq \\ & \ln\left|I_{N_r} + (\mathcal{L}_{i,j_\mathsf{D}}(\mathbf{V}_{i,j_\mathsf{D}}))^2\Psi^{-1}_{i,j_\mathsf{D}}(\mathbf{V}_\mathsf{D}, \mathbf{V}_\mathsf{U}, \boldsymbol{\alpha}_{i,j_\mathsf{D}})\right|, \end{aligned} \tag{3}$$

where $\mathcal{L}_{i,j_\mathsf{D}}(\mathbf{V}_{i,j_\mathsf{D}}) \triangleq H_{i,i,j_\mathsf{D}}\mathbf{V}_{i,j_\mathsf{D}}$ and

$$\Psi_{i,j_\mathsf{D}}(\mathbf{V}_\mathsf{D}, \mathbf{V}_\mathsf{U}, \boldsymbol{\alpha}_{i,j_\mathsf{D}}) \triangleq \bar{\Psi}_{i,j_\mathsf{D}}(\mathbf{V}_\mathsf{D}, \mathbf{V}_\mathsf{U}) + (\sigma_c^2/\boldsymbol{\alpha}_{i,j_\mathsf{D}})I_{N_r} \tag{4}$$

with the *downlink interference covariance mapping*

$$\begin{aligned} \bar{\Psi}_{i,j_\mathsf{D}}(\mathbf{V}_\mathsf{D}, \mathbf{V}_\mathsf{U}) \triangleq & \sum_{(m,\ell_\mathsf{D})\in\mathcal{S}_1\setminus(i,j_\mathsf{D})} (H_{m,i,j_\mathsf{D}}\mathbf{V}_{m,\ell_\mathsf{D}})^2 \\ & + \sum_{\ell_\mathsf{U}\in\mathcal{U}} (H_{i,j_\mathsf{D},\ell_\mathsf{U}}\mathbf{V}_{i,\ell_\mathsf{U}})^2 + \sigma_\mathsf{D} I_{N_r}. \end{aligned} \tag{5}$$

The harvested energy at UE (i, j_D) is

$$E_{i,j_\mathsf{D}}(\mathbf{V}_\mathsf{D}, \mathbf{V}_\mathsf{U}, \boldsymbol{\alpha}_{i,j_\mathsf{D}}) = \zeta_{i,j_\mathsf{D}}(1 - \boldsymbol{\alpha}_{i,j_\mathsf{D}})\langle\Phi_{i,j_\mathsf{D}}(\mathbf{V}_\mathsf{D}, \mathbf{V}_\mathsf{U})\rangle, \tag{6}$$

with the *downlink signal covariance mapping*

$$\begin{aligned} \Phi_{i,j_\mathsf{D}}(\mathbf{V}_\mathsf{D}, \mathbf{V}_\mathsf{U}) \triangleq & \sum_{(m,\ell_\mathsf{D})\in\mathcal{S}_1} (H_{m,i,j_\mathsf{D}}\mathbf{V}_{m,\ell_\mathsf{D}})^2 \\ & + \sum_{\ell_\mathsf{U}\in\mathcal{U}} (H_{i,j_\mathsf{D},\ell_\mathsf{U}}\mathbf{V}_{i,\ell_\mathsf{U}})^2 + \sigma_\mathsf{D}^2 I_{N_r}. \end{aligned} \tag{7}$$

In the UL channel, the received signal at BS i is expressed as

$$\begin{aligned} y_i \triangleq & \underbrace{\sum_{\ell_\mathsf{U}\in\mathcal{U}} H_{i,\ell_\mathsf{U},i}\mathbf{V}_{i,\ell_\mathsf{U}}s_{i,\ell_\mathsf{U}}}_{\text{desired signal}} \\ & + \underbrace{\sum_{m\in\mathcal{I}\setminus\{i\}}\sum_{\ell_\mathsf{U}\in\mathcal{U}} H_{m,\ell_\mathsf{U},i}\mathbf{V}_{m,\ell_\mathsf{U}}s_{m,\ell_\mathsf{U}}}_{\text{UL interference}} \\ & + \underbrace{\sum_{m\in\mathcal{I}\setminus\{i\}} H^{\mathcal{B}}_{m,i}\sum_{j_\mathsf{D}\in\mathcal{D}}\mathbf{V}_{m,j_\mathsf{D}}s_{m,j_\mathsf{D}}}_{\text{DL intercell interference}} + \underbrace{n_i^{SI}}_{\text{residual SI}} + n_i, \end{aligned} \tag{8}$$

where $H_{m,\ell_\mathsf{U},i} \in \mathbb{C}^{N_2 \times N_r}$ and $H^{\mathcal{B}}_{m,i} \in \mathbb{C}^{N_2 \times N_1}$ are the channel matrices from ULU (m, ℓ_U) to BS i and from BS

m to BS i, respectively; n_i is the additive white circularly symmetric complex Gaussian noise with variance σ_{U}^2; n_i^{SI} is the residual SI (after self-interference cancellation) at BS i and depends on the transmit power of BS i. Specifically, n_i^{SI} is modelled as the additive white circularly symmetric complex Gaussian noise with variance $\sigma_{SI}^2 \sum_{\ell_{\mathsf{D}} \in \mathcal{D}} ||\mathbf{V}_{i,\ell_{\mathsf{D}}}||^2$ [29], where the SI level σ_{SI}^2 is the ratio of the average SI powers after and before the SI cancellation process.

Following [14], [16], [26], the optimal minimum mean square error - Successive interference cancellation (MMSE-SIC) decoder is applied at BSs. Therefore, the achievable uplink throughput at BS i is given as [30]

$$f_i(\mathbf{V}_{\mathsf{D}}, \mathbf{V}_{\mathsf{U}}) \triangleq \ln \left| I_{N_2} + (\mathcal{L}_i(\mathbf{V}_{\mathsf{U}_i}))^2 \Psi_i^{-1}(\mathbf{V}_{\mathsf{D}}, \mathbf{V}_{\mathsf{U}}) \right|, \quad (9)$$

where $\mathbf{V}_{\mathsf{U}_i} \triangleq [\mathbf{V}_{i,\ell_{\mathsf{U}}}]_{\ell_{\mathsf{U}} \in \mathcal{U}}$ and $\mathcal{L}_i(\mathbf{V}_{\mathsf{U}i}) \triangleq \underset{U}{\left[H_{i,1_{\mathsf{U}},i}\mathbf{V}_{i,1_{\mathsf{U}}}, H_{i,2_{\mathsf{U}},i}\mathbf{V}_{i,2_{\mathsf{U}}}, \ldots, H_{i,U_{\mathsf{U}},i}\mathbf{V}_{i,U_{\mathsf{U}}}\right]}$, which means that $(\mathcal{L}_i(\mathbf{V}_{\mathsf{U}i}))^2 = \sum_{\ell=1}^{U} (H_{i,\ell_{\mathsf{U}},i}\mathbf{V}_{i,\ell_{\mathsf{U}}})^2$, and

$$\Psi_i(\mathbf{V}_{\mathsf{D}}, \mathbf{V}_{\mathsf{U}}) \triangleq \bar{\Psi}_i^U(\mathbf{V}_{\mathsf{U}}) + \bar{\Psi}_i^{SI}(\mathbf{V}_{\mathsf{D}}) \quad (10)$$

with *uplink interference covariance mapping*

$$\bar{\Psi}_i^U(\mathbf{V}_{\mathsf{U}}) \triangleq \sum_{m \in \mathcal{I} \setminus \{i\}} \sum_{\ell_{\mathsf{U}} \in \mathcal{U}} (H_{m,\ell_{\mathsf{U}},i}\mathbf{V}_{m,\ell_{\mathsf{U}}})^2 + \sum_{m \in \mathcal{I} \setminus \{i\}} H_{m,i}^{\mathcal{B}} \left(\sum_{j_{\mathsf{D}} \in \mathcal{D}} (\mathbf{V}_{m,j_{\mathsf{D}}})^2 \right) (H_{m,i}^{\mathcal{B}})^H + \sigma_{\mathsf{U}}^2 I_{N_2} \quad (11)$$

and *SI covariance mapping*

$$\bar{\Psi}_i^{SI}(\mathbf{V}_{\mathsf{D}}) \triangleq \sigma_{SI}^2 \sum_{\ell_{\mathsf{D}} \in \mathcal{D}} ||\mathbf{V}_{i,\ell_{\mathsf{D}}}||^2 I_{N_2}. \quad (12)$$

We consider the design problem

$$\begin{aligned}
\max_{\mathbf{V}_{\mathsf{D}}, \mathbf{V}_{\mathsf{U}}, \boldsymbol{\alpha}} \mathcal{P}_1(\mathbf{V}_{\mathsf{D}}, \mathbf{V}_{\mathsf{U}}, \boldsymbol{\alpha}) &\triangleq \sum_{i \in \mathcal{I}} f_i(\mathbf{V}_{\mathsf{D}}, \mathbf{V}_{\mathsf{U}}) \\
&+ \sum_{(i,j_{\mathsf{D}}) \in \mathcal{S}_1} f_{i,j_{\mathsf{D}}}(\mathbf{V}_{\mathsf{D}}, \mathbf{V}_{\mathsf{U}}, \boldsymbol{\alpha}_{i,j_{\mathsf{D}}}) \quad \text{s.t.} && (13a)\\
0 < \boldsymbol{\alpha}_{i,j_{\mathsf{D}}} &< 1, (i,j_{\mathsf{D}}) \in \mathcal{S}_1, && (13b)\\
\sum_{(i,j_{\mathsf{D}}) \in \mathcal{S}_1} ||\mathbf{V}_{i,j_{\mathsf{D}}}||^2 &+ \sum_{(i,j_{\mathsf{U}}) \in \mathcal{S}_2} ||\mathbf{V}_{i,j_{\mathsf{U}}}||^2 \leq P, && (13c)\\
\sum_{j_{\mathsf{D}} \in \mathcal{D}} ||\mathbf{V}_{i,j_{\mathsf{D}}}||^2 &\leq P_i, \forall i \in \mathcal{I}, && (13d)\\
||\mathbf{V}_{i,j_{\mathsf{U}}}||^2 &\leq P_{i,j_{\mathsf{U}}}, \forall (i,j_{\mathsf{U}}) \in \mathcal{S}_2, && (13e)\\
\langle \Phi_{i,j_{\mathsf{D}}}(\mathbf{V}_{\mathsf{D}}, \mathbf{V}_{\mathsf{U}}) \rangle &\geq e_{i,j_{\mathsf{D}}}^{\min} / \zeta_{i,j_{\mathsf{D}}}(1 - \boldsymbol{\alpha}_{i,j_{\mathsf{D}}}), \\
&\forall (i,j_{\mathsf{D}}) \in \mathcal{S}_1, && (13f)\\
f_i(\mathbf{V}_{\mathsf{D}}, \mathbf{V}_{\mathsf{U}}) &\geq r_i^{\mathsf{U},\min}, \forall i \in \mathcal{I} && (13g)\\
f_{i,j_{\mathsf{D}}}(\mathbf{V}_{\mathsf{D}}, \mathbf{V}_{\mathsf{U}}, \boldsymbol{\alpha}_{i,j_{\mathsf{D}}}) &\geq r_{i,j_{\mathsf{D}}}^{\mathsf{D},\min}, \forall (i,j_{\mathsf{D}}) \in \mathcal{S}_1. && (13h)
\end{aligned}$$

In the formulation (13), all channel matrices in the downlink equation (1) and uplink (8) are assumed to be known by using the channel reciprocity, feedback and learning mechanisms (see e.g. [31]). The convex constraints (13d) and (13e) specify the maximum transmit power available at the BSs and the ULUs whereas (13c) limits the total transmit power of the whole network. The nonconvex constraints (13f), (13g) and (13h) represent QoS guarantee, where $e_{i,j_{\mathsf{D}}}^{\min}, r_i^{\mathsf{U},\min}$ and $r_{i,j_{\mathsf{D}}}^{\mathsf{D},\min}$ are the minimum harvested energy required by DLU (i,j_{D}), the minimum data throughput required by BS i and the minimum data throughput required by DLU (i,j_{D}). In comparison to [16] for FD non-EH-enable networks, the UL throughput function $f_i(\mathbf{V}_{\mathsf{D}}, \mathbf{V}_{\mathsf{U}})$ in (9) is the same, where the DL throughput function $f_{i,j_{\mathsf{D}}}(\mathbf{V}_{\mathsf{D}}, \mathbf{V}_{\mathsf{U}}, \boldsymbol{\alpha}_{i,j_{\mathsf{D}}})$ is now additionally dependent on the SP variable $\boldsymbol{\alpha}_{i,j_{\mathsf{D}}}$, is decoupled in (5) and thus does not add more difficulty as we will show now. We also show that the nonconvex EH constraints (13f) can easily be innerly approximated.

Under the definitions,

$$\begin{aligned}
\mathcal{M}_{i,j_{\mathsf{D}}}(\mathbf{V}_{\mathsf{D}}, \mathbf{V}_{\mathsf{U}}, \boldsymbol{\alpha}_{i,j_{\mathsf{D}}}) &\triangleq (\mathcal{L}_{i,j_{\mathsf{D}}}(\mathbf{V}_{i,j_{\mathsf{D}}}))^2 \\
&\quad + \Psi_{i,j_{\mathsf{D}}}(\mathbf{V}_{\mathsf{D}}, \mathbf{V}_{\mathsf{U}}, \boldsymbol{\alpha}_{i,j_{\mathsf{D}}}) && (14)\\
&\succeq \Psi_{i,j_{\mathsf{D}}}(\mathbf{V}_{\mathsf{D}}, \mathbf{V}_{\mathsf{U}}, \boldsymbol{\alpha}_{i,j_{\mathsf{D}}}), && (15)\\
\mathcal{M}_i(\mathbf{V}_{\mathsf{D}}, \mathbf{V}_{\mathsf{U}}) &\triangleq (\mathcal{L}_i(\mathbf{V}_{\mathsf{U}i}))^2 + \Psi_i(\mathbf{V}_{\mathsf{D}}, \mathbf{V}_{\mathsf{U}}) && (16)\\
&\succeq \Psi_i(\mathbf{V}_{\mathsf{D}}, \mathbf{V}_{\mathsf{U}}), && (17)
\end{aligned}$$

by applying Theorem 1 as in [16], we obtain the following concave quadratic minorants of throughput functions $f_{i,j_{\mathsf{D}}}(\mathbf{V}_{\mathsf{D}}, \mathbf{V}_{\mathsf{U}}, \boldsymbol{\alpha}_{i,j_{\mathsf{D}}})$ and $f_i(\mathbf{V}_{\mathsf{D}}^{(\kappa)}, \mathbf{V}_{\mathsf{U}}^{(\kappa)})$ at $(V_{\mathsf{D}}^{(\kappa)}, V_{\mathsf{U}}^{(\kappa)}, \alpha^{(\kappa)}) \triangleq ([V_{i,j_{\mathsf{D}}}^{(\kappa)}]_{(i,j_{\mathsf{D}}) \in \mathcal{S}_1}, [V_{i,\ell_{\mathsf{U}}}^{(\kappa)}]_{(i,\ell_{\mathsf{U}}) \in \mathcal{S}_2}, [\alpha_{i,j_{\mathsf{D}}}^{(\kappa)}]_{(i,j_{\mathsf{D}}) \in \mathcal{S}_1})$:

$$\begin{aligned}
\Theta_{i,j_{\mathsf{D}}}^{(\kappa)}(\mathbf{V}_{\mathsf{D}}, \mathbf{V}_{\mathsf{U}}, \boldsymbol{\alpha}_{i,j_{\mathsf{D}}}) &\triangleq \\
a_{i,j_{\mathsf{D}}}^{(\kappa)} + 2\Re \left\{ \langle \mathcal{A}_{i,j_{\mathsf{D}}}^{(\kappa)}, \mathcal{L}_{i,j_{\mathsf{D}}}(\mathbf{V}_{i,j_{\mathsf{D}}}) \rangle \right\} \\
- \langle \mathcal{B}_{i,j_{\mathsf{D}}}^{(\kappa)}, \mathcal{M}_{i,j_{\mathsf{D}}}(\mathbf{V}_{\mathsf{D}}, \mathbf{V}_{\mathsf{U}}, \boldsymbol{\alpha}_{i,j_{\mathsf{D}}}) \rangle && (18)
\end{aligned}$$

and

$$\begin{aligned}
\Theta_i^{(\kappa)}(\mathbf{V}_{\mathsf{D}}, \mathbf{V}_{\mathsf{U}}) &\triangleq \\
a_i^{(\kappa)} + 2\Re \left\{ \langle \mathcal{A}_i^{(\kappa)}, \mathcal{L}_i(\mathbf{V}_{\mathsf{U}_i}) \rangle \right\} - \langle \mathcal{B}_i^{(\kappa)}, \mathcal{M}_i(\mathbf{V}_{\mathsf{D}}, \mathbf{V}_{\mathsf{U}}) \rangle, && (19)
\end{aligned}$$

where

$$\begin{aligned}
0 > a_{i,j_{\mathsf{D}}}^{(\kappa)} &\triangleq f_{i,j_{\mathsf{D}}}(V_{\mathsf{D}}^{(\kappa)}, V_{\mathsf{U}}^{(\kappa)}, \alpha_{i,j_{\mathsf{D}}}^{(\kappa)}) \\
-\Re \left\{ \langle \Psi_{i,j_{\mathsf{D}}}^{-1}(V_{\mathsf{D}}^{(\kappa)}, V_{\mathsf{U}}^{(\kappa)}) \mathcal{L}_{i,j_{\mathsf{D}}}(V_{i,j_{\mathsf{D}}}^{(\kappa)}), \mathcal{L}_{i,j_{\mathsf{D}}}(V_{i,j_{\mathsf{D}}}^{(\kappa)}) \rangle \right\}, \\
\mathcal{A}_{i,j_{\mathsf{D}}}^{(\kappa)} &= \Psi_{i,j_{\mathsf{D}}}^{-1}(V_{\mathsf{D}}^{(\kappa)}, V_{\mathsf{U}}^{(\kappa)}, \alpha_{i,j_{\mathsf{D}}}^{(\kappa)}) \mathcal{L}_{i,j_{\mathsf{D}}}(V_{i,j_{\mathsf{D}}}^{(\kappa)}), \\
0 \preceq \mathcal{B}_{i,j_{\mathsf{D}}}^{(\kappa)} &= \Psi_{i,j_{\mathsf{D}}}^{-1}(V_{\mathsf{D}}^{(\kappa)}, V_{\mathsf{U}}^{(\kappa)}, \alpha_{i,j_{\mathsf{D}}}^{(\kappa)}) \\
&\quad - \mathcal{M}_{i,j_{\mathsf{D}}}^{-1}(V_{\mathsf{D}}^{(\kappa)}, V_{\mathsf{U}}^{(\kappa)}, \alpha_{i,j_{\mathsf{D}}}^{(\kappa)}), && (20)
\end{aligned}$$

and

$$\begin{aligned}
0 > a_i^{(\kappa)} &= f_i(V_{\mathsf{D}}^{(\kappa)}, V_{\mathsf{U}}^{(\kappa)}) \\
-\Re \left\{ \langle \Psi_i^{-1}(V_{\mathsf{D}}^{(\kappa)}, V_{\mathsf{U}}^{(\kappa)}) \mathcal{L}_i(V_i^{(\kappa)}), \mathcal{L}_i(V_i^{(\kappa)}) \rangle \right\}, \\
\mathcal{A}_i^{(\kappa)} &= \Psi_i^{-1}(V_{\mathsf{D}}^{(\kappa)}, V_{\mathsf{U}}^{(\kappa)}) \mathcal{L}_i(V_{\mathsf{U}_i}^{(\kappa)}), \\
0 \preceq \mathcal{B}_i^{(\kappa)} &= \Psi_i^{-1}(V_{\mathsf{D}}^{(\kappa)}, V_{\mathsf{U}}^{(\kappa)}) \\
&\quad - \mathcal{M}_i^{-1}(V_{\mathsf{D}}^{(\kappa)}, V_{\mathsf{U}}^{(\kappa)}). && (21)
\end{aligned}$$

To handle the nonconvex EH constraints (13f), we define an affine function $\phi_{i,j_{\mathsf{D}}}^{(\kappa)}(\mathbf{V}_{\mathsf{D}}, \mathbf{V}_{\mathsf{U}})$ as the first-order approximation

Algorithm 1 Path-following algorithm for PS sum throughput maximization (13)

Initialization: Set $\kappa := 0$, and choose a feasible point $(V_{\mathsf{D}}^{(0)}, V_{\mathsf{U}}^{(0)}, \alpha^{(0)})$ that satisfies (13b)-(13h).

κ-th iteration: Solve (23) for an optimal solution $(V_{\mathsf{D}}^{*}, V_{\mathsf{U}}^{*}, \alpha^{*})$ and set $\kappa := \kappa + 1$, $(V_{\mathsf{D}}^{(\kappa)}, V_{\mathsf{U}}^{(\kappa)}, \alpha^{(\kappa)}) := (V_{\mathsf{D}}^{*}, V_{\mathsf{U}}^{*}, \alpha^{*})$ and calculate $\mathcal{P}_1(V_{\mathsf{D}}^{(\kappa)}, V_{\mathsf{U}}^{(\kappa)}, \alpha^{(\kappa)})$. Stop if $\Big|\Big(\mathcal{P}_1(V_{\mathsf{D}}^{(\kappa)}, V_{\mathsf{U}}^{(\kappa)}, \alpha^{(\kappa)}) - \mathcal{P}_1(V_{\mathsf{D}}^{(\kappa-1)}, V_{\mathsf{U}}^{(\kappa-1)}, \alpha^{(\kappa-1)})\Big) / \mathcal{P}_1(V_{\mathsf{D}}^{(\kappa-1)}, V_{\mathsf{U}}^{(\kappa-1)}, \alpha^{(\kappa-1)})\Big| \leq \epsilon$.

of the convex function $\langle \Phi_{i,j_{\mathsf{D}}}(\mathbf{V}_{\mathsf{D}}, \mathbf{V}_{\mathsf{U}})\rangle$ at $(V_{\mathsf{D}}^{(\kappa)}, V_{\mathsf{U}}^{(\kappa)})$:

$$\begin{aligned}\phi_{i,j_{\mathsf{D}}}^{(\kappa)}(\mathbf{V}_{\mathsf{D}}, \mathbf{V}_{\mathsf{U}}) \triangleq & -\langle \Phi_{i,j_{\mathsf{D}}}(V_{\mathsf{D}}^{(\kappa)}, V_{\mathsf{U}}^{(\kappa)})\rangle \\ & + 2\Re\{\sum_{(m,\ell_{\mathsf{D}})\in\mathcal{S}_1} \langle H_{m,i,j_{\mathsf{D}}} V_{m,\ell_{\mathsf{D}}}^{(\kappa)} \mathbf{V}_{m,\ell_{\mathsf{D}}} H_{m,i,j_{\mathsf{D}}}^{H}\rangle\} \\ & + 2\Re\{\sum_{\ell_{\mathsf{U}}\in\mathcal{U}} \langle H_{i,i_{\mathsf{D}},\ell_{\mathsf{U}}} V_{i,\ell_{\mathsf{U}}}^{(\kappa)} \mathbf{V}_{i,\ell_{\mathsf{U}}}^{H} H_{i,i_{\mathsf{D}},\ell_{\mathsf{U}}}^{H}\rangle\} + 2\sigma_{\mathsf{D}}^2 N_r, \end{aligned} \tag{22}$$

which is an minorant of $\langle \Phi_{i,j_{\mathsf{D}}}(\mathbf{V}_{\mathsf{D}}, \mathbf{V}_{\mathsf{U}})\rangle$ at $(V_{\mathsf{D}}^{(\kappa)}, V_{\mathsf{U}}^{(\kappa)})$ [28].

We now address the nonconvex problem (13) by successively solving its following inner approximation:

$$\begin{aligned}\max_{\mathbf{V}_{\mathsf{D}},\mathbf{V}_{\mathsf{U}},\boldsymbol{\alpha}} \ & \mathcal{P}_1^{(\kappa)}(\mathbf{V}_{\mathsf{D}}, \mathbf{V}_{\mathsf{U}}, \boldsymbol{\alpha}) \triangleq \sum_{i\in\mathcal{I}} \Theta_i^{(\kappa)}(\mathbf{V}_{\mathsf{D}}, \mathbf{V}_{\mathsf{U}}) \\ & \qquad + \sum_{(i,j_{\mathsf{D}})\in\mathcal{S}_1} \Theta_{i,j_{\mathsf{D}}}^{(\kappa)}(\mathbf{V}_{\mathsf{D}}, \mathbf{V}_{\mathsf{U}}, \boldsymbol{\alpha}_{i,j_{\mathsf{D}}}) && \text{(23a)} \\ & \qquad \text{s.t.} \quad (13\text{b}) - (13\text{e}) && \text{(23b)} \\ & \phi_{i,j_{\mathsf{D}}}^{(\kappa)}(\mathbf{V}_{\mathsf{D}}, \mathbf{V}_{\mathsf{U}}) \geq e_{i,j_{\mathsf{D}}}^{\min}/\zeta_{i,j_{\mathsf{D}}}(1-\boldsymbol{\alpha}_{i,j_{\mathsf{D}}}), \\ & \qquad \forall (i,j_{\mathsf{D}}) \in \mathcal{S}_1, && \text{(23c)} \\ & \Theta_i^{(\kappa)}(\mathbf{V}_{\mathsf{D}}, \mathbf{V}_{\mathsf{U}}) \geq r_i^{\mathsf{U},\min}, \forall i \in \mathcal{I}, && \text{(23d)} \\ & \Theta_{i,j_{\mathsf{D}}}^{(\kappa)}(\mathbf{V}_{\mathsf{D}}, \mathbf{V}_{\mathsf{U}}, \boldsymbol{\alpha}_{i,j_{\mathsf{D}}}) \geq r_{i,j_{\mathsf{D}}}^{\mathsf{D},\min}, \forall (i,j_{\mathsf{D}}) \in \mathcal{S}_1. && \text{(23e)}\end{aligned}$$

Initializing from $(V_{\mathsf{D}}^{(\kappa)}, V_{\mathsf{U}}^{(\kappa)}, \alpha^{(\kappa)})$ being feasible point to (13), the optimal solution $(V_{\mathsf{D}}^{(\kappa+1)}, V_{\mathsf{U}}^{(\kappa+1)}, \alpha^{(\kappa+1)})$ of convex program (23) is feasible to the nonconvex program (13) and it is better than $(V_{\mathsf{D}}^{(\kappa)}, V_{\mathsf{U}}^{(\kappa)}, \alpha^{(\kappa)})$:

$$\begin{aligned}\mathcal{P}_1(V_{\mathsf{D}}^{(\kappa+1)}, V_{\mathsf{U}}^{(\kappa+1)}, \alpha^{(\kappa+1)}) & \geq \\ \mathcal{P}_1^{(\kappa)}(V_{\mathsf{D}}^{(\kappa+1)}, V_{\mathsf{U}}^{(\kappa+1)}, \alpha^{(\kappa+1)}) & \geq && \text{(24)} \\ \mathcal{P}_1^{(\kappa)}(V_{\mathsf{D}}^{(\kappa)}, V_{\mathsf{U}}^{(\kappa)}, \alpha^{(\kappa)}) & = && \text{(25)} \\ \mathcal{P}_1(V_{\mathsf{D}}^{(\kappa)}, V_{\mathsf{U}}^{(\kappa)}, \alpha^{(\kappa)}), & && \text{(26)}\end{aligned}$$

where the inequality (24) and the equality (26) follow from the fact that $\mathcal{P}_1^{(\kappa)}$ is a minorant of $\mathcal{P}_1$ while the inequality (25) follows from the fact that $(V_{\mathsf{D}}^{(\kappa+1)}, V_{\mathsf{U}}^{(\kappa+1)}, \alpha^{(\kappa+1)})$ and $(V_{\mathsf{D}}^{(\kappa)}, V_{\mathsf{U}}^{(\kappa)}, \alpha^{(\kappa)})$ are the optimal solution and feasible point of (23), respectively. This generates a sequence $\{(V_{\mathsf{D}}^{(\kappa)}, V_{\mathsf{U}}^{(\kappa)}, \alpha^{(\kappa)})\}$ of feasible and improved points which converge to a local optimum of (13) after finitely many iterations [16].

The proposed path-following procedure that solves problem (13) is summarized in Algorithm 1. To find a feasible initial point $(V_{\mathsf{D}}^{(0)}, V_{\mathsf{U}}^{(0)}, \alpha^{(0)})$ meeting the nonconvex constraints (13f)-(13h) we consider the following problem:

$$\begin{aligned}\max_{\mathbf{V}_{\mathsf{D}},\mathbf{V}_{\mathsf{U}},\boldsymbol{\alpha}} & \mathcal{P}_{1,f}(\mathbf{V}_{\mathsf{D}}, \mathbf{V}_{\mathsf{U}}, \boldsymbol{\alpha}) \triangleq \\ \min_{(i,j_{\mathsf{D}})\in\mathcal{S}_1} & \Big\{\Phi_{i,j_{\mathsf{D}}}(\mathbf{V}_{\mathsf{D}}, \mathbf{V}_{\mathsf{U}}) - \frac{e_{i,j_{\mathsf{D}}}^{\min}}{\zeta_{i,j_{\mathsf{D}}}(1-\boldsymbol{\alpha}_{i,j_{\mathsf{D}}})}, \\ & f_{i,j_{\mathsf{D}}}(\mathbf{V}_{\mathsf{D}}, \mathbf{V}_{\mathsf{U}}, \boldsymbol{\alpha}) - r_{i,i_{\mathsf{D}}}^{\min}, f_i(\mathbf{V}_{\mathsf{D}}, \mathbf{V}_{\mathsf{U}}) - r_i^{\min}\Big\} \\ & \text{s.t.} \quad (13\text{b}) - (13\text{e}).\end{aligned} \tag{27}$$

Initialized by a $(V_{\mathsf{D}}^{(0)}, V_{\mathsf{U}}^{(0)}, \alpha^{(0)})$ feasible to the convex constraints (13b)-(13e), an iterative point $(V_{\mathsf{D}}^{(\kappa+1)}, V_{\mathsf{U}}^{(\kappa+1)}, \alpha^{(\kappa+1)})$ for $\kappa = 0, 1, \ldots,$ is generated as the optimal solution of the following convex maximin program:

$$\begin{aligned}\max_{\mathbf{V}_{\mathsf{D}},\mathbf{V}_{\mathsf{U}},\boldsymbol{\alpha}} & \mathcal{P}_{1,f}^{(\kappa)}(\mathbf{V}_{\mathsf{D}}, \mathbf{V}_{\mathsf{U}}, \boldsymbol{\alpha}) \triangleq \\ \min_{(i,j_{\mathsf{D}})\in\mathcal{S}_1} & \Big\{\phi_{i,j_{\mathsf{D}}}^{(\kappa)}(\mathbf{V}_{\mathsf{D}}, \mathbf{V}_{\mathsf{U}}) - \frac{e_{i,j_{\mathsf{D}}}^{\min}}{\zeta_{i,j_{\mathsf{D}}}(1-\boldsymbol{\alpha}_{i,j_{\mathsf{D}}})}, \\ & \langle \Theta_{i,j_{\mathsf{D}}}^{(\kappa)}(\mathbf{V}_{\mathsf{D}}, \mathbf{V}_{\mathsf{U}}, \boldsymbol{\alpha}) - r_{i,i_{\mathsf{D}}}^{\min}, \Theta_i^{(\kappa)}(\mathbf{V}_{\mathsf{D}}, \mathbf{V}_{\mathsf{U}}) - r_i^{\min}, \Big\} \\ & \text{s.t} \quad (13\text{b}) - (13\text{e}).\end{aligned} \tag{28}$$

which terminates upon reaching

$$\begin{aligned}& f_{i,j_{\mathsf{D}}}(V_{\mathsf{D}}^{(\kappa)}, V_{\mathsf{U}}^{(\kappa)}, \alpha^{(\kappa)}) \geq r_{i,i_{\mathsf{D}}}^{\min}, f_i(V_{\mathsf{D}}^{(\kappa)}, V_{\mathsf{U}}^{(\kappa)}) \geq r_i^{\min}, \\ & \langle \Phi_{i,j_{\mathsf{D}}}(V_{\mathsf{D}}^{(\kappa)}, V_{\mathsf{U}}^{(\kappa)})\rangle \geq \frac{e_{i,j_{\mathsf{D}}}^{\min}}{\zeta_{i,j_{\mathsf{D}}}(1-\boldsymbol{\alpha}_{i,j_{\mathsf{D}}})}, \ \forall (i,j_{\mathsf{D}}) \in \mathcal{S}_1\end{aligned}$$

to satisfy (13b)-(13h).

In parallel, we consider the following transmission strategy to configure FD BSs to operate in the HD mode. Here, all antennas $N = N_1 + N_2$ at each BS are used to serve all the DLUs in the downlink and all the ULUs in the uplink using half time slots, where DLUs are allowed to harvest energy from ULUs. The problem can be formulated as

$$\begin{aligned}\max_{\mathbf{V}_{\mathsf{D}},\mathbf{V}_{\mathsf{U}},\boldsymbol{\alpha}} & \frac{1}{2}\Big[\sum_{(i,j_{\mathsf{D}})\in\mathcal{S}_1} f_{i,j_{\mathsf{D}}}(\mathbf{V}_{\mathsf{D}}, 0_{\mathsf{U}}, \boldsymbol{\alpha}_{i,j_{\mathsf{D}}}) \\ & \qquad + \sum_{i\in\mathcal{I}} f_i(0_{\mathsf{D}}, \mathbf{V}_{\mathsf{U}})\Big] && \text{(29a)} \\ & \text{s.t.} \quad (13\text{b}), (13\text{c}), (13\text{d}), (13\text{e}), \\ & \frac{1}{2}(E_{i,j_{\mathsf{D}}}(\mathbf{V}_{\mathsf{D}}, 0_{\mathsf{U}}, \boldsymbol{\alpha}_{i,j_{\mathsf{D}}}) + E_{i,j_{\mathsf{D}}}(0_{\mathsf{D}}, \mathbf{V}_{\mathsf{U}}, 0)) \geq \\ & \qquad e_{i,j_{\mathsf{D}}}^{\min}, \forall (i,j_{\mathsf{D}}) \in \mathcal{S}_1, && \text{(29b)} \\ & \frac{1}{2} f_i(0_{\mathsf{D}}, \mathbf{V}_{\mathsf{U}}) \geq r_i^{\mathsf{U},\min}, \forall i \in \mathcal{I} && \text{(29c)} \\ & \frac{1}{2} f_{i,j_{\mathsf{D}}}(\mathbf{V}_{\mathsf{D}}, 0_{\mathsf{U}}, \boldsymbol{\alpha}_{i,j_{\mathsf{D}}}) \geq r_{i,j_{\mathsf{D}}}^{\mathsf{D},\min}, \forall (i,j_{\mathsf{D}}) \in \mathcal{S}_1, && \text{(29d)}\end{aligned}$$

where 0_{D} and 0_{U} are zero quantity of the same dimension with $\mathbf{V}_{\mathsf{D}}$ and $\mathbf{V}_{\mathsf{U}}$. In (29), DLU (i, j_{D}) uses $(1-\boldsymbol{\alpha}_{i,j_{\mathsf{D}}})$ of the received signal during DL transmission and the whole received signal during UL transmission for EH as formulated in (29b). The main difference between (13) and (29) is in (29b) where the harvested energy from UL transmission at DLU (i, j_{D}) does not multiply with $\boldsymbol{\alpha}_{i,j_{\mathsf{D}}}$. The constraint (29b) can be recast as

$$\langle \Phi_{i,j_{\mathsf{D}}}(\mathbf{V}_{\mathsf{D}}, 0_{\mathsf{U}})\rangle + \frac{\langle \Phi_{i,j_{\mathsf{D}}}(0_{\mathsf{D}}, \mathbf{V}_{\mathsf{U}})\rangle}{(1-\boldsymbol{\alpha}_{i,j_{\mathsf{D}}})} \geq \frac{2e_{i,j_{\mathsf{D}}}^{\min}}{\zeta_{i,j_{\mathsf{D}}}(1-\boldsymbol{\alpha}_{i,j_{\mathsf{D}}})}.$$

Define the following convex function:

$$\Lambda_{i,j_\mathsf{D}}(\mathbf{V}_\mathsf{U},\boldsymbol{\alpha}_{i,j_\mathsf{D}}) \triangleq \frac{\langle \Phi_{i,j_\mathsf{D}}(0_\mathsf{D},\mathbf{V}_\mathsf{U})\rangle}{(1-\boldsymbol{\alpha}_{i,j_\mathsf{D}})} = \frac{\langle \sum_{\ell_\mathsf{U}\in\mathcal{U}}(H_{i,j_\mathsf{D},\ell_\mathsf{U}}\mathbf{V}_{i,\ell_\mathsf{U}})^2 + \sigma_\mathsf{D}^2 I_{N_r}\rangle}{1-\boldsymbol{\alpha}_{i,j_\mathsf{D}}}, \quad (30)$$

with its first-order approximation

$$\Lambda_{i,j_\mathsf{D}}^{(\kappa)}(\mathbf{V}_\mathsf{U},1-\boldsymbol{\alpha}_{i,j_\mathsf{D}}) \triangleq \frac{2\Re\{\langle \sum_{\ell_\mathsf{U}\in\mathcal{U}}(H_{i,j_\mathsf{D},\ell_\mathsf{U}}\mathbf{V}_{i,\ell_\mathsf{U}})(H_{i,j_\mathsf{D},\ell_\mathsf{U}}V_{i,\ell_\mathsf{U}}^{(\kappa)})^H\rangle\}}{1-\alpha_{i,j_\mathsf{D}}^{(\kappa)}} - \frac{\langle \sum_{\ell_\mathsf{U}\in\mathcal{U}}(H_{i,j_\mathsf{D},\ell_\mathsf{U}}V_{i,\ell_\mathsf{U}}^{(\kappa)})^2 + \sigma_\mathsf{D}^2 I_{N_r}\rangle}{(1-\alpha_{i,j_\mathsf{D}}^{(\kappa)})^2}(1-\boldsymbol{\alpha}_{i,j_\mathsf{D}}), \quad (31)$$

which is its minorant at $(V_\mathsf{D}^{(\kappa)}, V_\mathsf{U}^{(\kappa)}, \alpha^{(\kappa)})$.

Algorithm 1 can be used with the following convex program solved for κ-iteration:

$$\max_{\mathbf{V}_\mathsf{D},\mathbf{V}_\mathsf{U},\boldsymbol{\alpha}} \frac{1}{2}\Big[\sum_{(i,j_\mathsf{D})\in\mathcal{S}_1}\Theta_{i,j_\mathsf{D}}^{(\kappa)}(\mathbf{V}_\mathsf{D},0_\mathsf{U},\boldsymbol{\alpha}_{i,j_\mathsf{D}}) + \sum_{i\in\mathcal{I}}\Theta_i^{(\kappa)}(0_\mathsf{D},\mathbf{V}_\mathsf{U},0)\Big] \quad (32a)$$

$$\text{s.t. (13b), (13c), (13d), (13e)},$$

$$\phi_{i,j_\mathsf{D}}^{(\kappa)}(\mathbf{V}_\mathsf{D},0_\mathsf{U}) + \Lambda_{i,j_\mathsf{D}}^{(\kappa)}(\mathbf{V}_\mathsf{U},1-\boldsymbol{\alpha}_{i,j_\mathsf{D}}) \geq \frac{2e_{i,j_\mathsf{D}}^{\min}}{\zeta_{i,j_\mathsf{D}}(1-\boldsymbol{\alpha}_{i,j_\mathsf{D}})}, \forall (i,j_\mathsf{D})\in\mathcal{S}_1, \quad (32b)$$

$$\frac{1}{2}\Theta_i^{(\kappa)}(0_\mathsf{D},\mathbf{V}_\mathsf{U}) \geq r_i^{\mathsf{U},\min}, \forall i\in\mathcal{I} \quad (32c)$$

$$\frac{1}{2}\Theta_{i,j_\mathsf{D}}^{(\kappa)}(\mathbf{V}_\mathsf{D},0_\mathsf{U},\boldsymbol{\alpha}_{i,j_\mathsf{D}}) \geq r_{i,j_\mathsf{D}}^{\mathsf{D},\min}, \forall (i,j_\mathsf{D})\in\mathcal{S}_1, \quad (32d)$$

where $\phi_{i,j_\mathsf{D}}^{(\kappa)}(\mathbf{V}_\mathsf{D},0_\mathsf{U})$ and $\Theta_{i,j_\mathsf{D}}^{(\kappa)}(\mathbf{V}_\mathsf{D},0_\mathsf{U},\boldsymbol{\alpha}_{i,j_\mathsf{D}})$ are defined by (22) and (18) with both $\mathbf{V}_\mathsf{U}$ and $V_\mathsf{U}^{(\kappa)}$ replaced by 0_U, while $\Theta_i^{(\kappa)}(0_\mathsf{D},\mathbf{V}_\mathsf{U})$ is defined by (19) with both $\mathbf{V}_\mathsf{D}$ and $V_\mathsf{D}^{(\kappa)}$ replaced by 0_D.

Problems (23), (28) and (32) involve $n = 2(N_1 d_1 ID + N_r d_2 IU) + ID$ scalar real decision variables and $m = 5ID+IU+2I+1$ quadratic constraints so their computational complexity is $O(n^2 m^{2.5} + m^{3.5})$.

III. EH-enabled FD MU-MIMO by TS

A much easier implementation is time splitting $0 < \boldsymbol{\alpha} < 1$ in downlink transmission where $(1-\boldsymbol{\alpha})$ time is used for DL energy transfer and $\boldsymbol{\alpha}$ time is used for DL information transmission. In this section, we define $\mathbf{V}_\mathsf{D}^I \triangleq [\mathbf{V}_{i,j_\mathsf{D}}^I]_{(i,j_\mathsf{D})\in\mathcal{S}_1}, \mathbf{V}_\mathsf{D}^E \triangleq [\mathbf{V}_{i,j_\mathsf{D}}^E]_{(i,j_\mathsf{D})\in\mathcal{S}_1}$ and redefine the notation $\mathbf{V}_\mathsf{D} \triangleq [\mathbf{V}_\mathsf{D}^I, \mathbf{V}_\mathsf{D}^E]$ where $\mathbf{V}_{i,j_\mathsf{D}}^I$ and $\mathbf{V}_{i,j_\mathsf{D}}^E$ are the information precoding matrix for ID and energy precoding matrix for EH, respectively. The received signal at DLU (i,j_D) for EH is

$$y_{i,j_\mathsf{D}}^E \triangleq \sum_{(m,\ell_\mathsf{D})\in\mathcal{S}_1} H_{m,i,j_\mathsf{D}}\mathbf{V}_{m,\ell_\mathsf{D}}^E s_{m,\ell_\mathsf{D}}^E + \underbrace{\sum_{\ell_\mathsf{U}\in\mathcal{U}} H_{i,j_\mathsf{D},\ell_\mathsf{U}}\mathbf{V}_{i,\ell_\mathsf{U}}s_{i,\ell_\mathsf{U}}}_{\text{UL intracell interference}} + n_{j_\mathsf{D}}, \quad (33)$$

where s_{m,ℓ_D}^E is the energy signal sent for $(1-\boldsymbol{\alpha})$ time. With the definition (6), the harvested energy is

$$E_{i,j_\mathsf{D}}(\mathbf{V}_\mathsf{D}^E,\mathbf{V}_\mathsf{U},\boldsymbol{\alpha}) = \zeta_{i,j_\mathsf{D}}(1-\boldsymbol{\alpha})\langle\Phi_{i,j_\mathsf{D}}(\mathbf{V}_\mathsf{D}^E,\mathbf{V}_\mathsf{U})\rangle,$$

where the downlink signal covariance mapping $\Phi_{i,j_\mathsf{D}}(.,.)$ is defined from (7).
Similarly to (1), the signal received at DLU (i,j_D) during the information transmission in time fraction $\boldsymbol{\alpha}$ is

$$y_{i,j_\mathsf{D}}^I \triangleq \underbrace{H_{i,i,j_\mathsf{D}}\mathbf{V}_{i,j_\mathsf{D}}s_{i,j_\mathsf{D}}^I}_{\text{desired signal}} + \underbrace{\sum_{(m,\ell_\mathsf{D})\in\mathcal{S}_1\setminus(i,j_\mathsf{D})} H_{m,i,j_\mathsf{D}}\mathbf{V}_{m,\ell_\mathsf{D}}s_{m,\ell_\mathsf{D}}^I}_{\text{DL interference}} + \underbrace{\sum_{\ell_\mathsf{U}\in\mathcal{U}} H_{i,j_\mathsf{D},\ell_\mathsf{U}}\mathbf{V}_{i,\ell_\mathsf{U}}s_{i,\ell_\mathsf{U}}}_{\text{UL intracell interference}} + n_{i,j_\mathsf{D}}, \quad (34)$$

where s_{m,ℓ_D}^I is the information signal intended for DLU (m,ℓ_D). The ID throughput at DLU (i,j_D) is then given as $\boldsymbol{\alpha} f_{i,j_\mathsf{D}}(\mathbf{V})$, where

$$f_{i,j_\mathsf{D}}(\mathbf{V}_\mathsf{D}^I,\mathbf{V}_\mathsf{U}) = \ln\Big|I_{N_r} + (\mathcal{L}_{i,j_\mathsf{D}}(\mathbf{V}_{i,j_\mathsf{D}}^I))^2\bar{\Psi}_{i,j_\mathsf{D}}^{-1}(\mathbf{V}_\mathsf{D}^I,\mathbf{V}_\mathsf{U})\Big|, \quad (35)$$

with the downlink interference covariance mapping $\bar{\Psi}(.,.)$ defined from (5).
The uplink throughput at the BS is

$$f_i(\mathbf{V}_\mathsf{D},\mathbf{V}_\mathsf{U},\boldsymbol{\alpha}) \triangleq \ln\Big|I_{N_2} + (\mathcal{L}_i(\mathbf{V}_{\mathsf{U}_i}))^2 s\Psi_i^{-1}(\mathbf{V}_\mathsf{D},\mathbf{V}_\mathsf{U},\boldsymbol{\alpha})\Big|, \quad (36)$$

where $\mathcal{L}_i(\mathbf{V}_{\mathsf{U}_i})$ is already defined from (9) but

$$\Psi_i(\mathbf{V}_\mathsf{D},\mathbf{V}_\mathsf{U},\boldsymbol{\alpha}) \triangleq \bar{\Psi}_i^U(\mathbf{V}_\mathsf{U}) + \bar{\Psi}_i^{TSI}(\mathbf{V}_\mathsf{D},\boldsymbol{\alpha}) \quad (37)$$

with the uplink interference covariance mapping $\bar{\Psi}_i^U(.)$ defined by (11) and the time-splitting SI covariance mapping

$$\bar{\Psi}_i^{TSI}(\mathbf{V}_\mathsf{D},\boldsymbol{\alpha}) \triangleq \sigma_{SI}^2\sum_{j_\mathsf{D}\in\mathcal{D}}\Big((1-\boldsymbol{\alpha})||\mathbf{V}_{i,j_\mathsf{D}}^E||^2 + \boldsymbol{\alpha}||\mathbf{V}_{i,j_\mathsf{D}}^I||^2\Big)I_{N_2}. \quad (38)$$

The problem of maximizing the network total throughput under throughput QoS and EH constraints is the following:

$$\max_{\mathbf{V}_\mathsf{D},\mathbf{V}_\mathsf{U},\boldsymbol{\alpha}} \ \mathcal{P}_2(\mathbf{V}_\mathsf{D},\mathbf{V}_\mathsf{U},\boldsymbol{\alpha}) \triangleq$$

$$\sum_{(i,j_\mathsf{D})\in\mathcal{S}_1} \Big(\boldsymbol{\alpha} f_{i,j_\mathsf{D}}(\mathbf{V}_\mathsf{D}^I,\mathbf{V}_\mathsf{U}) + f_i(\mathbf{V}_\mathsf{D},\mathbf{V}_\mathsf{U},\boldsymbol{\alpha})\Big) \tag{39a}$$

$$\text{s.t.} \quad 0<\boldsymbol{\alpha}<1, \tag{39b}$$

$$||\mathbf{V}_{i,j_\mathsf{U}}||^2 \le P_{i,j_\mathsf{U}}, \forall (i,j_\mathsf{U})\in\mathcal{S}_2, \tag{39c}$$

$$\sum_{(i,j_\mathsf{D})\in\mathcal{S}_1} \Big((1-\boldsymbol{\alpha})||\mathbf{V}_{i,j_\mathsf{D}}^E||^2 + \boldsymbol{\alpha}||\mathbf{V}_{i,j_\mathsf{D}}^I||^2\Big) + \sum_{(i,j_\mathsf{U})\in\mathcal{S}_2} ||\mathbf{V}_{i,j_\mathsf{U}}||^2 \le P, \tag{39d}$$

$$\sum_{j_\mathsf{D}\in\mathcal{D}} \Big((1-\boldsymbol{\alpha})||\mathbf{V}_{i,j_\mathsf{D}}^E||^2 + \boldsymbol{\alpha}||\mathbf{V}_{i,j_\mathsf{D}}^I||^2\Big) \le P_i, \forall i\in\mathcal{I}, \tag{39e}$$

$$f_i(\mathbf{V}_\mathsf{D},\mathbf{V}_\mathsf{U},\boldsymbol{\alpha}) \ge r_i^{\mathsf{U},\min}, \forall i\in\mathcal{I}, \tag{39f}$$

$$\boldsymbol{\alpha} f_{i,j_\mathsf{D}}(\mathbf{V}_\mathsf{D}^I,\mathbf{V}_\mathsf{U}) \ge r_{i,j_\mathsf{D}}^{\mathsf{D},\min}, \forall (i,j_\mathsf{D})\in\mathcal{S}_1, \tag{39g}$$

$$E_{i,j_\mathsf{D}}(\mathbf{V}_\mathsf{D}^E,\mathbf{V}_\mathsf{U},\boldsymbol{\alpha}) \ge e_{i,j_\mathsf{D}}^{\min}, \forall (i,j_\mathsf{D})\in\mathcal{S}_1. \tag{39h}$$

Constraints (39c), (39d) and (39e) limits the transmit power of each ULU, the whole network and each BS, respectively. Constraints (39h) ensures that each DLUs harvest more than a threshold whereas constraints (39f) and (39g) guarantee the throughput QoS at BSs and DLUs, respectively. The key difficulty in problem (39) is to handle the time splitting factor $\boldsymbol{\alpha}$ that is coupled with the objective functions and other variables. Using the variable change $\boldsymbol{\rho}=1/\boldsymbol{\alpha}$, which satisfies the convex constraint

$$\boldsymbol{\rho} > 1, \tag{40}$$

problem (39) is equivalent to

$$\max_{\mathbf{V}_\mathsf{D},\mathbf{V}_\mathsf{U},\boldsymbol{\rho}>0} \ \mathcal{P}_2(\mathbf{V}_\mathsf{D},\mathbf{V}_\mathsf{U},\boldsymbol{\rho}) \triangleq$$

$$\sum_{(i,j_\mathsf{D})\in\mathcal{S}_1} f_{i,j_\mathsf{D}}(\mathbf{V}_\mathsf{D}^I,\mathbf{V}_\mathsf{U})/\boldsymbol{\rho} + \sum_{i\in\mathcal{I}} f_i(\mathbf{V}_\mathsf{D},\mathbf{V}_\mathsf{U},1/\boldsymbol{\rho}) \tag{41a}$$

$$\text{s.t. } (40),(39c),$$

$$\sum_{(i,j_\mathsf{D})\in\mathcal{S}_1} \Big(||\mathbf{V}_{i,j_\mathsf{D}}^E||^2 + ||\mathbf{V}_{i,j_\mathsf{D}}^I||^2/\boldsymbol{\rho}\Big) + \sum_{(i,j_\mathsf{U})\in\mathcal{S}_2} ||\mathbf{V}_{i,j_\mathsf{U}}||^2 \le P + \sum_{(i,j_\mathsf{D})\in\mathcal{S}_1} ||\mathbf{V}_{i,j_\mathsf{D}}^E||^2/\boldsymbol{\rho}, \tag{41b}$$

$$\sum_{j_\mathsf{D}\in\mathcal{D}} \Big(||\mathbf{V}_{i,j_\mathsf{D}}^E||^2 + ||\mathbf{V}_{i,j_\mathsf{D}}^I||^2/\boldsymbol{\rho}\Big) \le P_i + \sum_{j_\mathsf{D}\in\mathcal{D}} ||\mathbf{V}_{i,j_\mathsf{D}}^E||^2/\boldsymbol{\rho}, \ \forall i\in\mathcal{I}, \tag{41c}$$

$$E_{i,j_\mathsf{D}}(\mathbf{V}_\mathsf{D}^E,\mathbf{V}_\mathsf{U},1/\boldsymbol{\rho}) \ge e_{i,j_\mathsf{D}}^{\min}, \forall (i,j_\mathsf{D})\in\mathcal{S}_1, \tag{41d}$$

$$f_i(\mathbf{V}_\mathsf{D},\mathbf{V}_\mathsf{U},1/\boldsymbol{\rho}) \ge r_i^{\mathsf{U},\min}, \forall i\in\mathcal{I}, \tag{41e}$$

$$f_{i,j_\mathsf{D}}(\mathbf{V}_\mathsf{D}^I,\mathbf{V}_\mathsf{U})/\boldsymbol{\rho} \ge r_{i,j_\mathsf{D}}^{\mathsf{D},\min}, \forall (i,j_\mathsf{D})\in\mathcal{S}_1. \tag{41f}$$

Problem (41) is much more difficult computationally than (13). Firstly, the DL throughput is now the multiplication of data throughput and the portion of time $1/\boldsymbol{\rho}$. Secondly, the SI in UL throughput is also coupled with $1/\boldsymbol{\rho}$. Finally, the power constraints (41b), (41c) are also coupled with $1/\boldsymbol{\rho}$. Therefore, the objective function (41a) and constraints (41b)-(41f) are all nonconvex and cannot be addressed as in (13). In the following, we will develop the new minorants of the DL throughput function and UL throughput function.

Firstly, we address a lower approximation for each $f_{i,j_\mathsf{D}}(\mathbf{V}_\mathsf{D}^I,\mathbf{V}_\mathsf{U})/\boldsymbol{\rho}$ in (41a) and (41f). Recalling the definition (35) of $f_{i,j_\mathsf{D}}(\mathbf{V}_\mathsf{D}^I,\mathbf{V}_\mathsf{U})$ we introduce

$$\mathcal{M}_{i,j_\mathsf{D}}(\mathbf{V}_\mathsf{D}^I,\mathbf{V}_\mathsf{U}) \triangleq (\mathcal{L}_{i,j_\mathsf{D}}(\mathbf{V}_{i,j_\mathsf{D}}))^2 + \bar{\Psi}_{i,j_\mathsf{D}}(\mathbf{V}_\mathsf{D},\mathbf{V}_\mathsf{U}),$$

to have its following minorant at $(V_\mathsf{D}^{(\kappa)},V_\mathsf{U}^{(\kappa)})$:

$$\Theta_{i,j_\mathsf{D}}^{(\kappa)}(\mathbf{V}_\mathsf{D}^I,\mathbf{V}_\mathsf{U}) \triangleq a_{i,j_\mathsf{D}}^{(\kappa)} + 2\Re\Big\{\langle \mathcal{A}_{i,j_\mathsf{D}}^{(\kappa)}, \mathcal{L}_{i,j_\mathsf{D}}(\mathbf{V}_{i,j_\mathsf{D}}^I)\rangle\Big\} - \langle \mathcal{B}_{i,j_\mathsf{D}}^{(\kappa)}, \mathcal{M}_{i,j_\mathsf{D}}(\mathbf{V}_\mathsf{D}^I,\mathbf{V}_\mathsf{U})\rangle, \tag{42}$$

where similarly to (20)

$$\begin{aligned} 0 > a_{i,j_\mathsf{D}}^{(\kappa)} &= f_{i,j_\mathsf{D}}(V_\mathsf{D}^{(\kappa)},V_\mathsf{U}^{(\kappa)}) \\ -\Re\Big\{\langle \bar{\Psi}_{i,j_\mathsf{D}}^{-1}(V_\mathsf{D}^{(\kappa)},V_\mathsf{U}^{(\kappa)})\mathcal{L}_{i,j_\mathsf{D}}(V_{i,j_\mathsf{D}}^{(\kappa)}), \mathcal{L}_{i,j_\mathsf{D}}(V_{i,j_\mathsf{D}}^{(\kappa)})\rangle\Big\}&, \\ \mathcal{A}_{i,j_\mathsf{D}}^{(\kappa)} = \bar{\Psi}_{i,j_\mathsf{D}}^{-1}(V_\mathsf{D}^{(\kappa)},V_\mathsf{U}^{(\kappa)})\mathcal{L}_{i,j_\mathsf{D}}(V_{i,j_\mathsf{D}}^{(\kappa)}),& \\ 0 \preceq \mathcal{B}_{i,j_\mathsf{D}}^{(\kappa)} = \bar{\Psi}_{i,j_\mathsf{D}}^{-1}(V_\mathsf{D}^{(\kappa)},V_\mathsf{U}^{(\kappa)}) - \mathcal{M}_{i,j_\mathsf{D}}^{-1}(V_\mathsf{D}^{(\kappa)},V_\mathsf{U}^{(\kappa)})&. \end{aligned} \tag{43}$$

A minorant of $f_{i,j_\mathsf{D}}(\mathbf{V}_\mathsf{D}^I,\mathbf{V}_\mathsf{U})/\boldsymbol{\rho}$ is $\Theta_{i,j_\mathsf{D}}^{(\kappa)}(\mathbf{V}_\mathsf{D}^I,\mathbf{V}_\mathsf{U})/\boldsymbol{\rho}$ but it is still not concave. As $f_{i,j_\mathsf{D}}(\mathbf{V}_\mathsf{D}^I,\mathbf{V}_\mathsf{U})>0$ it is obvious that its lower bound $\Theta_{i,j_\mathsf{D}}^{(\kappa)}(\mathbf{V}_\mathsf{D}^I,\mathbf{V}_\mathsf{U})$ is meaningful for $(\mathbf{V}_\mathsf{D}^I,\mathbf{V}_\mathsf{U})$ such that

$$\Theta_{i,j_\mathsf{D}}^{(\kappa)}(\mathbf{V}_\mathsf{D}^I,\mathbf{V}_\mathsf{U}) \ge 0, \ (i,j_\mathsf{D})\in\mathcal{S}_1 \tag{44}$$

which particularly implies

$$\Re\Big\{\Big\langle (\mathcal{A}_{i,j_\mathsf{D}}^{(\kappa)}, \mathcal{L}_{i,j_\mathsf{D}}(\mathbf{V}_{i,j_\mathsf{D}}^I)\Big\rangle\Big\} \ge 0, \ (i,j_\mathsf{D})\in\mathcal{S}_1. \tag{45}$$

Under (45), we have

$$\frac{\Re\Big\{\langle \mathcal{A}_{i,j_\mathsf{D}}^{(\kappa)}, \mathcal{L}_{i,j_\mathsf{D}}(\mathbf{V}_{i,j_\mathsf{D}}^I)\rangle\Big\}}{\boldsymbol{\rho}} \ge 2b_{i,j_\mathsf{D}}^{(\kappa)}\sqrt{\Re\Big\{\langle \mathcal{A}_{i,j_\mathsf{D}}^{(\kappa)}, \mathcal{L}_{i,j_\mathsf{D}}(\mathbf{V}_{i,j_\mathsf{D}}^I)\rangle\Big\}} - c_{i,j_\mathsf{D}}^{(\kappa)}\boldsymbol{\rho} \tag{46}$$

for

$$\begin{aligned} 0 < b_{i,j_\mathsf{D}}^{(\kappa)} &= \frac{\sqrt{\langle \mathcal{A}_{i,j_\mathsf{D}}^{(\kappa)}, \mathcal{L}_{i,j_\mathsf{D}}(V_{i,j_\mathsf{D}}^{I,(\kappa)})\rangle}}{\rho^{(\kappa)}}, \\ 0 < c_{i,j_\mathsf{D}}^{(\kappa)} &= (b_{i,j_\mathsf{D}}^{(\kappa)})^2. \end{aligned} \tag{47}$$

Therefore, the following concave function

$$g_{i,j_\mathsf{D}}^{(\kappa)}(\mathbf{V}_\mathsf{D}^I,\mathbf{V}_\mathsf{U},\boldsymbol{\rho}) \triangleq \frac{a_{i,j_\mathsf{D}}^{(\kappa)}}{\boldsymbol{\rho}} + 4b_{i,j_\mathsf{D}}^{(\kappa)}\sqrt{\Re\Big\{\langle \mathcal{A}_{i,j_\mathsf{D}}^{(\kappa)}, \mathcal{L}_{i,j_\mathsf{D}}(\mathbf{V}_{i,j_\mathsf{D}}^I)\rangle\Big\}} - 2c_{i,j_\mathsf{D}}^{(\kappa)}\boldsymbol{\rho} - \frac{\langle \mathcal{B}^{(\kappa)}, \mathcal{M}_{i,j_\mathsf{D}}(\mathbf{V}_\mathsf{D}^I,\mathbf{V}_\mathsf{U})\rangle}{\boldsymbol{\rho}} \tag{48}$$

is a minorant of $f_{i,j_\mathsf{D}}(\mathbf{V}_\mathsf{D}^I,\mathbf{V}_\mathsf{U})/\boldsymbol{\rho}$ at $(V_\mathsf{D}^{I,(\kappa)},V_\mathsf{U}^{(\kappa)},\rho^{(\kappa)})$.

Next, we address a lower approximation of $f_i(\mathbf{V}_\mathsf{D},\mathbf{V}_\mathsf{U},1/\boldsymbol{\rho})$ in (41a), (41e). Recalling the definition (36) of $f_i(\mathbf{V}_\mathsf{D},\mathbf{V}_\mathsf{U},1/\boldsymbol{\rho})$ we introduce

$$\mathcal{M}_i(\mathbf{V}_\mathsf{D},\mathbf{V}_\mathsf{U},\boldsymbol{\rho}) \triangleq (\mathcal{L}_i(\mathbf{V}_{\mathsf{U}i}))^2 + \bar{\Psi}_i^U(\mathbf{V}_\mathsf{U}) + \bar{\Psi}_i^{TSI}(\mathbf{V}_\mathsf{D},1/\boldsymbol{\rho}), \tag{49}$$

for $\bar{\Psi}_i^{TSI}(\mathbf{V}_\mathsf{D}, 1/\boldsymbol{\rho})$ defined from (38) as

$$\begin{aligned}\bar{\Psi}_i^{TSI}(\mathbf{V}_\mathsf{D}, 1/\boldsymbol{\rho}) =&\sigma_{SI}^2 \sum_{j_\mathsf{D}\in\mathcal{D}} \Big(||\mathbf{V}_{i,j_\mathsf{D}}^E||^2 \\ &+ \frac{1}{\boldsymbol{\rho}}||\mathbf{V}_{i,j_\mathsf{D}}^I||^2 - \frac{1}{\boldsymbol{\rho}}||\mathbf{V}_{i,j_\mathsf{D}}^E||^2\Big) I_{N_2}, \quad (50)\end{aligned}$$

to have its following minorant at $(V_\mathsf{D}^{(\kappa)}, V_\mathsf{U}^{(\kappa)}, \rho^{(\kappa)})$:

$$\begin{aligned}\Theta_i^{(\kappa)}(\mathbf{V}_\mathsf{D}, \mathbf{V}_\mathsf{U}, \boldsymbol{\rho}) \triangleq& a_i^{(\kappa)} + 2\Re\Big\{\langle \mathcal{A}_i^{(\kappa)}, \mathcal{L}_i(\mathbf{V}_{\mathsf{U}_i})\rangle\Big\} \\ &- \langle \mathcal{B}_i^{(\kappa)}, \mathcal{M}_i(\mathbf{V}_\mathsf{D}, \mathbf{V}_\mathsf{U}, \boldsymbol{\rho})\rangle, \quad (51)\end{aligned}$$

where similarly to (21)

$$\begin{aligned}0 > a_i^{(\kappa)} &= f_i(V_\mathsf{D}^{(\kappa)}, V_\mathsf{U}^{(\kappa)}) \\ -\Re\Big\{\langle \Psi_i^{-1}(V_\mathsf{D}^{(\kappa)}, V_\mathsf{U}^{(\kappa)})\mathcal{L}_i(V_i^{(\kappa)}), \mathcal{L}_i(V_i^{(\kappa)})\rangle\Big\}&, \\ \mathcal{A}_i^{(\kappa)} &= \Psi_i^{-1}(V_\mathsf{D}^{(\kappa)}, V_\mathsf{U}^{(\kappa)})\mathcal{L}_i(V_{\mathsf{U}_i}^{(\kappa)}), \\ 0 \preceq \mathcal{B}_i^{(\kappa)} &= \Psi_i^{-1}(V_\mathsf{D}^{(\kappa)}, V_\mathsf{U}^{(\kappa)}) - \mathcal{M}_i^{-1}(V_\mathsf{D}^{(\kappa)}, V_\mathsf{U}^{(\kappa)}).\end{aligned} \quad (52)$$

Function $\Theta_i^{(\kappa)}(\mathbf{V}_\mathsf{D}, \mathbf{V}_\mathsf{U}, \boldsymbol{\rho})$ is not concave due to the term $\bar{\Psi}_i^{TSI}(\mathbf{V}_\mathsf{D}, 1/\boldsymbol{\rho})$ defined by (50). However, the following *matrix inequality* holds true:

$$\begin{aligned}\frac{1}{\boldsymbol{\rho}}||\mathbf{V}_{i,j_\mathsf{D}}^E||^2 I_{N_2} \succeq& (\frac{2}{\rho^{(\kappa)}}\Re\{\langle V_{i,j_\mathsf{D}}^{E,(\kappa)}, \mathbf{V}_{i,j_\mathsf{D}}^E\rangle\} \\ &- \frac{||V_{i,j_\mathsf{D}}^{E,(\kappa)}||^2}{(\rho^{(\kappa)})^2}\boldsymbol{\rho}) I_{N_2}, \quad (53)\end{aligned}$$

which yields the matrix inequality

$$\begin{aligned}\mathcal{M}_i(\mathbf{V}_\mathsf{D}, \mathbf{V}_\mathsf{U}, \boldsymbol{\rho}) \succeq& \\ \mathcal{M}_i^{(\kappa)}(\mathbf{V}_\mathsf{D}, \mathbf{V}_\mathsf{U}, \boldsymbol{\rho}) \triangleq& \\ (\mathcal{L}_i(\mathbf{V}_{\mathsf{U}i}))^2 + \bar{\Psi}_i^U(\mathbf{V}_\mathsf{U}) + \sigma_{SI}^2 \Big(||\mathbf{V}_{i,j_\mathsf{D}}^E||^2 + \frac{1}{\boldsymbol{\rho}}||\mathbf{V}_{i,j_\mathsf{D}}^I||^2& \\ - \frac{2}{\rho^{(\kappa)}}\Re\{\langle V_{i,j_\mathsf{D}}^{E,(\kappa)}, \mathbf{V}_{i,j_\mathsf{D}}^E\rangle\} + \frac{||V_{i,j_\mathsf{D}}^{E,(\kappa)}||^2}{(\rho^{(\kappa)})^2}\boldsymbol{\rho}\Big) I_{N_2}.&\end{aligned}$$

As $\mathcal{B}_i^{(\kappa)} \succeq 0$ by (52), we then have

$$\langle \mathcal{B}_i^{(\kappa)}, \mathcal{M}_i(\mathbf{V}_\mathsf{D}, \mathbf{V}_\mathsf{U}, \boldsymbol{\rho})\rangle \geq \langle \mathcal{B}_i^{(\kappa)}, \mathcal{M}_i^{(\kappa)}(\mathbf{V}_\mathsf{D}, \mathbf{V}_\mathsf{U}, \boldsymbol{\rho})\rangle$$

so a concave minorant of both $f_i(\mathbf{V}_\mathsf{D}, \mathbf{V}_\mathsf{U}, 1/\boldsymbol{\rho})$ and $\Theta^{(\kappa)}(\mathbf{V}_\mathsf{D}, \mathbf{V}_\mathsf{U}, \boldsymbol{\rho})$ is

$$\begin{aligned}\tilde{\Theta}_i^{(\kappa)}(\mathbf{V}_\mathsf{D}, \mathbf{V}_\mathsf{U}, \boldsymbol{\rho}) \triangleq& a_i^{(\kappa)} + 2\Re\Big\{\langle \mathcal{A}_i^{(\kappa)}, \mathcal{L}_i(\mathbf{V}_{\mathsf{U}_i})\rangle\Big\} \\ &- \langle \mathcal{B}_i^{(\kappa)}, \mathcal{M}_i^{(\kappa)}(\mathbf{V}_\mathsf{D}, \mathbf{V}_\mathsf{U}, \boldsymbol{\rho})\rangle. \quad (54)\end{aligned}$$

Concerned with $||\mathbf{V}_{i,j_\mathsf{D}}^E||^2/\boldsymbol{\rho}$ in the right hand side (RHS) of (41b) and (41c), it follows from (53) that

$$\begin{aligned}||\mathbf{V}_{i,j_\mathsf{D}}^E||^2/\boldsymbol{\rho} \geq& \quad \gamma_{i,j_\mathsf{D}}^{(\kappa)}(\mathbf{V}_{i,j_\mathsf{D}}^E, \boldsymbol{\rho}) \\ \triangleq& \quad 2\Re\{\langle V_{i,j_\mathsf{D}}^{E,(\kappa)}, \mathbf{V}_{i,j_\mathsf{D}}^E\rangle\}/\rho^{(\kappa)} \\ &-\boldsymbol{\rho}||V_{i,j_\mathsf{D}}^{E,(\kappa)}||^2/(\rho^{(\kappa)})^2.\end{aligned}$$

We also have $\phi_{i,j_\mathsf{D}}^{(\kappa)}(\mathbf{V}_\mathsf{D}^E, \mathbf{V}_\mathsf{U})$ defined in (22) as a minorant of $\langle \Phi_{i,j_\mathsf{D}}(\mathbf{V}_\mathsf{D}^E, \mathbf{V}_\mathsf{U})\rangle$. We now address the nonconvex problem

Algorithm 2 Path-following algorithm for TS optimization problem (41)

Initialization: Set $\kappa := 0$, and choose a feasible point $(V_\mathsf{D}^{(0)}, V_\mathsf{U}^{(0)}, \alpha^{(0)})$ that satisfies (39b)-(39g). Set $\rho^{(0)} := 1/\alpha^{(0)}$.

κ-th iteration: Solve (55) for an optimal solution $(V_\mathsf{D}^*, V_\mathsf{U}^*, \rho^*)$ and set $\kappa := \kappa + 1$, $(V_\mathsf{D}^{(\kappa)}, V_\mathsf{U}^{(\kappa)}, \rho^{(\kappa)}) := (V_\mathsf{D}^*, V_\mathsf{U}^*, \rho^*)$ and calculate $\mathcal{P}_2(V_\mathsf{D}^{(\kappa)}, V_\mathsf{U}^{(\kappa)}, 1/\rho^{(\kappa)})$. Stop if $\left|\left(\mathcal{P}_2(x^{(\kappa)}) - \mathcal{P}_2(x^{(\kappa-1)})\right)/\mathcal{P}_2(x^{(\kappa-1)})\right| \leq \epsilon$, where $x^{(\kappa)} \triangleq (V_\mathsf{D}^{(\kappa)}, V_\mathsf{U}^{(\kappa)}, 1/\rho^{(\kappa)})$

(41) by successively solving its following innerly approximated convex program at κ-iteration:

$$\max_{\mathbf{V}_\mathsf{D}, \mathbf{V}_\mathsf{U}, \boldsymbol{\rho}>0} \mathcal{P}_2^{(\kappa)}(\mathbf{V}_\mathsf{D}, \mathbf{V}_\mathsf{U}, \boldsymbol{\rho}) \quad (55a)$$

$$\text{s.t. } (40), (39c), \quad (55b)$$

$$\sum_{(i,j_\mathsf{D})\in\mathcal{S}_1} \Big(||\mathbf{V}_{i,j_\mathsf{D}}^E||^2 + \frac{1}{\boldsymbol{\rho}}||\mathbf{V}_{i,j_\mathsf{D}}^I||^2\Big) +$$

$$\sum_{(i,j_\mathsf{U})\in\mathcal{S}_2} ||\mathbf{V}_{i,j_\mathsf{U}}||^2 \leq P + \sum_{(i,j_\mathsf{D})\in\mathcal{S}_1} \gamma_{i,j_\mathsf{D}}^{(\kappa)}(\mathbf{V}_{i,j_\mathsf{D}}^E, \boldsymbol{\rho}), \quad (55c)$$

$$\sum_{j_\mathsf{D}\in\mathcal{D}} \Big(||\mathbf{V}_{i,j_\mathsf{D}}^E||^2 + \frac{1}{\boldsymbol{\rho}}||\mathbf{V}_{i,j_\mathsf{D}}^I||^2\Big) \leq$$

$$P_i + \sum_{j_\mathsf{D}\in\mathcal{D}} \gamma_{i,j_\mathsf{D}}^{(\kappa)}(\mathbf{V}_{i,j_\mathsf{D}}^E, \boldsymbol{\rho}), \forall i \in \mathcal{I}, \quad (55d)$$

$$\phi_{i,j_\mathsf{D}}^{(\kappa)}(\mathbf{V}_\mathsf{D}^E, \mathbf{V}_\mathsf{U}) \geq e_{i,j_\mathsf{D}}^{\min}(1 + \frac{1}{\boldsymbol{\rho} - 1})/\zeta_{i,j_\mathsf{D}},$$

$$\forall (i, j_\mathsf{D}) \in \mathcal{S}_1, \quad (55e)$$

$$\tilde{\Theta}_i^{(\kappa)}(\mathbf{V}_\mathsf{D}, \mathbf{V}_\mathsf{U}, \boldsymbol{\rho}) \geq r_i^{\mathsf{U},\min}, \forall i \in \mathcal{I}, \quad (55f)$$

$$g_{i,j_\mathsf{D}}^{(\kappa)}(\mathbf{V}_\mathsf{D}^I, \mathbf{V}_\mathsf{U}, \boldsymbol{\rho}) \geq r_{i,j_\mathsf{D}}^{\mathsf{D},\min}. \forall (i, j_\mathsf{D}) \in \mathcal{S}_1. \quad (55g)$$

where $\mathcal{P}_2^{(\kappa)}(\mathbf{V}_\mathsf{D}, \mathbf{V}_\mathsf{U}, \boldsymbol{\rho}) \triangleq \sum_{i\in\mathcal{I}} \tilde{\Theta}_i^{(\kappa)}(\mathbf{V}_\mathsf{D}, \mathbf{V}_\mathsf{U}, \boldsymbol{\rho}) + \sum_{(i,j_\mathsf{D})\in\mathcal{S}_1} g_{i,j_\mathsf{D}}^{(\kappa)}(\mathbf{V}_\mathsf{D}^I, \mathbf{V}_\mathsf{U}, \boldsymbol{\rho})$.

A path-following procedure similar to Algorithm 1 can be applied to solve (41) as summarized in Algorithm 2. Thanks to the following relation, which is similar to (26):

$$\mathcal{P}_2(V_\mathsf{D}^{(\kappa+1)}, V_\mathsf{U}^{(\kappa+1)}, \rho^{(\kappa+1)}) \geq \mathcal{P}_2(V_\mathsf{D}^{(\kappa)}, V_\mathsf{U}^{(\kappa)}, \rho^{(\kappa)}), \quad (56)$$

Algorithm 2 improves feasible point at each iteration and then bring a local optimum after finitely many iterations.

To find an initial feasible point for Algorithm 2, we consider the following problem:

$$\begin{aligned}\max_{\mathbf{V}_\mathsf{D}, \mathbf{V}_\mathsf{U}, \boldsymbol{\rho}} \min_{(i,j_\mathsf{D})\in\mathcal{S}_1} \Big\{ & f_i(\mathbf{V}_\mathsf{D}, \mathbf{V}_\mathsf{U}, 1/\boldsymbol{\rho}) - r_i^{\min}, \\ & E_{i,j_\mathsf{D}}(\mathbf{V}_\mathsf{D}^E, \mathbf{V}_\mathsf{U}, 1/\boldsymbol{\rho}) - e_{i,j_\mathsf{D}}^{\min}, \\ & f_{i,j_\mathsf{D}}(\mathbf{V}_\mathsf{D}^I, \mathbf{V}_\mathsf{U})/\boldsymbol{\rho} - r_{i,i_\mathsf{D}}^{\min}\Big\} : \ (41b) - (41c)\end{aligned} \quad (57)$$

which can be addressed by successively solving the following convex maximin program:

$$\begin{aligned}\max_{\mathbf{V}_\mathsf{D}, \mathbf{V}_\mathsf{U}, \boldsymbol{\rho}} \min_{(i,j_\mathsf{D})\in\mathcal{S}_1} \Big\{ & g_{i,j_\mathsf{D}}^{(\kappa)}(\mathbf{V}_\mathsf{D}^I, \mathbf{V}_\mathsf{U}, \boldsymbol{\rho}) - r_{i,i_\mathsf{D}}^{\min}, \\ & \phi_{i,j_\mathsf{D}}^{(\kappa)}(\mathbf{V}_\mathsf{D}^E, \mathbf{V}_\mathsf{U}) - e_{i,j_\mathsf{D}}^{\min}(1 + \frac{1}{\boldsymbol{\rho} - 1})/\zeta_{i,j_\mathsf{D}}, \\ & \tilde{\Theta}_i^{(\kappa)}(\mathbf{V}_\mathsf{D}, \mathbf{V}_\mathsf{U}, \boldsymbol{\rho}) - r_i^{\min}\Big\} : (55b) - (55d),\end{aligned} \quad (58)$$

upon reaching $f_{i,j_\mathsf{D}}(V_\mathsf{D}^{I,(\kappa)}, V_\mathsf{U}^{(\kappa)}, \alpha^{(\kappa)}) \geq r_{i,i_\mathsf{D}}^{\min}$, $f_i(V_\mathsf{D}^{(\kappa)}, V_\mathsf{U}^{(\kappa)}, \alpha^{(\kappa)}) \geq r_i^{\min}$ and $E_{i,j_\mathsf{D}}(V_\mathsf{D}^{E,(\kappa)}, V_\mathsf{U}^{(\kappa)}, 1/\rho^{(\kappa)}) \geq e_{i,j_\mathsf{D}}^{\min}, \forall (i,j_\mathsf{D}) \in \mathcal{S}_1$.

For the system operating in HD mode, we apply the same transmission strategy as in Section II. Specifically, we consider the following problem:

$$\max_{\mathbf{V}_\mathsf{D}, \mathbf{V}_\mathsf{U}, \boldsymbol{\rho}} \frac{1}{2}[\sum_{(i,j_\mathsf{D})\in\mathcal{S}_1} \frac{1}{\boldsymbol{\rho}} f_{i,j_\mathsf{D}}(\mathbf{V}_\mathsf{D}, 0_\mathsf{U}) + \sum_{i\in\mathcal{I}} f_i(0_\mathsf{D}, \mathbf{V}_\mathsf{U}, 1)] \quad \text{s.t.} \quad (39b)-(39e) \tag{59a}$$

$$\frac{1}{2}(E_{i,j_\mathsf{D}}(\mathbf{V}_\mathsf{D}, 0_\mathsf{U}, 1/\boldsymbol{\rho}) + E_{i,j_\mathsf{D}}(0_\mathsf{D}, \mathbf{V}_\mathsf{U}, 1)) \geq, \quad e_{i,j_\mathsf{D}}^{\min} \ (i,j_\mathsf{D}) \in \mathcal{S}_1, \tag{59b}$$

$$\frac{1}{2\boldsymbol{\rho}} f_{i,j_\mathsf{D}}(\mathbf{V}_\mathsf{D}, 0_\mathsf{U}) \geq r_{i,j_\mathsf{D}}^{\mathsf{D},\min}, \forall (i,j_\mathsf{D}) \in \mathcal{S}_1, \tag{59c}$$

$$\frac{1}{2} f_i(0_\mathsf{D}, \mathbf{V}_\mathsf{U}, 1) \geq r_i^{\mathsf{U},\min}, \forall i \in \mathcal{I}. \tag{59d}$$

In (59), DLUs harvest energy for $(1-\boldsymbol{\alpha})$ of $1/2$ time slot during DL transmission and for the whole $1/2$ time slot during UL transmission as formulated in (59b). The constraint (59b) can be written by

$$\Xi_{i,j_\mathsf{D}}(\mathbf{V}_\mathsf{D}, \mathbf{V}_\mathsf{U}, \boldsymbol{\rho}) \geq \frac{2e_{i,j_\mathsf{D}}^{\min}}{\zeta_{i,j_\mathsf{D}}}(1 + \frac{1}{\boldsymbol{\rho}-1}), \tag{60}$$

for

$$\Xi_{i,j_\mathsf{D}}(\mathbf{V}_\mathsf{D}, \mathbf{V}_\mathsf{U}, \boldsymbol{\rho}) \triangleq \langle \Phi_{i,j_\mathsf{D}}(\mathbf{V}_\mathsf{D}, 0_\mathsf{U})\rangle + \langle \Phi_{i,j_\mathsf{D}}(0_\mathsf{D}, \mathbf{V}_\mathsf{U})\rangle + \frac{\langle \Phi_{i,j_\mathsf{D}}(0_\mathsf{D}, \mathbf{V}_\mathsf{U})\rangle}{\boldsymbol{\rho}-1}.$$

As Ξ_{i,j_D} is convex, its minorant is its first-order approximation at $(V_\mathsf{D}^{(\kappa)}, V_\mathsf{U}^{(\kappa)}, \rho^{(\kappa)})$:

$$\Xi_{i,j_\mathsf{D}}^{(\kappa)}(\mathbf{V}_\mathsf{D}, \mathbf{V}_\mathsf{U}, \boldsymbol{\rho}) = \phi_{i,j_\mathsf{D}}^{(\kappa)}(\mathbf{V}_\mathsf{D}, 0_\mathsf{U}) + \phi_{i,j_\mathsf{D}}^{(\kappa)}(0_\mathsf{D}, \mathbf{V}_\mathsf{U}) + \Lambda_{i,j_\mathsf{D}}^{(\kappa)}(\mathbf{V}_\mathsf{U}, \boldsymbol{\rho}-1),$$

for $\Lambda_{i,j_\mathsf{D}}^{(\kappa)}(.,.)$ defined by (31) and $\phi_{i,j_\mathsf{D}}^{(\kappa)}(0_\mathsf{D}, \mathbf{V}_\mathsf{U})$ defined from (22) with both $\mathbf{V}_\mathsf{U}$ and $V_\mathsf{U}^{(\kappa)}$ replaced by 0_U.

The problem (39) thus can be addressed via a path-following procedure similar to Algorithm 2 where the following convex program is solved for κ-iteration:

$$\max_{\mathbf{V}_\mathsf{D}, \mathbf{V}_\mathsf{U}, \boldsymbol{\rho}} \frac{1}{2}[\sum_{(i,j_\mathsf{D})\in\mathcal{S}_1} g_{i,j_\mathsf{D}}^{(\kappa)}(\mathbf{V}_\mathsf{D}^I, 0_\mathsf{U}, \boldsymbol{\rho}) + \sum_{i\in\mathcal{I}} \tilde{\Theta}_i^{(\kappa)}(0_\mathsf{D}, \mathbf{V}_\mathsf{U}, 1)] : (39b)-(39e) \tag{61a}$$

$$\Xi_{i,j_\mathsf{D}}^{(\kappa)}(\mathbf{V}_\mathsf{D}, \mathbf{V}_\mathsf{U}, \boldsymbol{\rho}) \geq \frac{2e_{i,j_\mathsf{D}}^{\min}}{\zeta_{i,j_\mathsf{D}}}(1 + \frac{1}{\boldsymbol{\rho}-1}), \tag{61b}$$

$$(i,j_\mathsf{D}) \in \mathcal{S}_1, \tag{61c}$$

$$\frac{1}{2} g_{i,j_\mathsf{D}}^{(\kappa)}(\mathbf{V}_\mathsf{D}, 0_\mathsf{U}, \boldsymbol{\rho}) \geq r_{i,j_\mathsf{D}}^{\mathsf{D},\min}, \forall (i,j_\mathsf{D}) \in \mathcal{S}_1, \tag{61d}$$

$$\frac{1}{2} \tilde{\Theta}_i^{(\kappa)}(0_\mathsf{D}, \mathbf{V}_\mathsf{U}, 1) \geq r_i^{\mathsf{U},\min}, \forall i \in \mathcal{I}, \tag{61e}$$

where $g_{i,j_\mathsf{D}}^{(\kappa)}(\mathbf{V}_\mathsf{D}^I, 0_\mathsf{U}, \boldsymbol{\rho})$ is defined by (48) with both $\mathbf{V}_\mathsf{U}$ and $V_\mathsf{U}^{(\kappa)}$ replaced by 0_U, while $\tilde{\Theta}_i^{(\kappa)}(0_\mathsf{D}, \mathbf{V}_\mathsf{U}, 0)$ is defined by (54) with both $\mathbf{V}_\mathsf{D}$ and $V_\mathsf{D}^{(\kappa)}$ replaced by 0_D and both $\boldsymbol{\rho}$ and $\rho^{(\kappa)}$ replaced by 1.

IV. Throughput QoS constrained energy-harvesting optimization

We will justify numerically that TS is not only easier implemented but performs better than PS for FD EH-enabled MU MIMO networks. This motivates us to consider the following EH optimization with TS, which has not been previously considered at all:

$$\max_{\mathbf{V}_\mathsf{D}, \mathbf{V}_\mathsf{U}, \boldsymbol{\alpha}} \mathcal{P}_3(\mathbf{V}, \boldsymbol{\alpha}) \triangleq \sum_{(i,j_\mathsf{D})\in\mathcal{S}_1} E_{i,j_\mathsf{D}}(\mathbf{V}_\mathsf{D}^E, \mathbf{V}_\mathsf{U}, \boldsymbol{\alpha}) \quad \text{s.t.} \quad (39b)-(39g). \tag{62}$$

By defining $\boldsymbol{\rho} = 1/\boldsymbol{\alpha}$, we firstly recast $E_{i,j_\mathsf{D}}(\mathbf{V}_\mathsf{D}^E, \mathbf{V}_\mathsf{U}, 1/\boldsymbol{\rho})$ as

$$E_{i,j_\mathsf{D}}(\mathbf{V}_\mathsf{D}^E, \mathbf{V}_\mathsf{U}, 1/\boldsymbol{\rho}) = \zeta_{i,j_\mathsf{D}}\Big(\langle \Phi_{i,j_\mathsf{D}}(\mathbf{V}_\mathsf{D}^E, \mathbf{V}_\mathsf{U})\rangle - Q_{i,j_\mathsf{D}}(\mathbf{V}_\mathsf{D}^E, \mathbf{V}_\mathsf{U}, \boldsymbol{\rho})\Big), \tag{63}$$

where $Q_{i,j_\mathsf{D}}(\mathbf{V}_\mathsf{D}^E, \mathbf{V}_\mathsf{U}, \boldsymbol{\rho}) \triangleq \frac{1}{\boldsymbol{\rho}}\langle \Phi_{i,j_\mathsf{D}}(\mathbf{V}_\mathsf{D}^E, \mathbf{V}_\mathsf{U})\rangle$ is a convex function. Recalling that $\phi_{i,j_\mathsf{D}}^{(\kappa)}(\mathbf{V}_\mathsf{D}^E, \mathbf{V}_\mathsf{U})$ defined in (22) is a minorant of $\langle \Phi_{i,j_\mathsf{D}}(\mathbf{V}_\mathsf{D}^E, \mathbf{V}_\mathsf{U})\rangle$, we can now address the nonconvex problem (62) by successively solving the following convex program at κ-iteration:

$$\max_{\mathbf{V}, \boldsymbol{\rho}} \sum_{(i,j_\mathsf{D})\in\mathcal{S}_1} \zeta_{i,j_\mathsf{D}}\Big(\phi_{i,j_\mathsf{D}}^{(\kappa)}(\mathbf{V}_\mathsf{D}^E, \mathbf{V}_\mathsf{U}) - Q_{i,j_\mathsf{D}}(\mathbf{V}_\mathsf{D}^E, \mathbf{V}_\mathsf{U}, \boldsymbol{\rho})\Big) \quad \text{s.t.} \quad (39c), (40), (55c), (55d), (55f), (55g). \tag{64}$$

A path-following procedure similar to Algorithm 2 can be applied to solve (62).

For the system operating in HD mode, the same transmission strategy as in Section II is applied. Specifically, we consider the following problem:

$$\max_{\mathbf{V}, \boldsymbol{\rho}} \sum_{(i,j_\mathsf{D})\in\mathcal{S}_1} \frac{1}{2}(E_{i,j_\mathsf{D}}(\mathbf{V}_\mathsf{D}^E, 0_\mathsf{U}, 1/\boldsymbol{\rho}) + E_{i,j_\mathsf{D}}(0_\mathsf{D}, \mathbf{V}_\mathsf{U}, 0)) \quad \text{s.t.} \quad (39c), (40), (39d), (39e), (59c), (59d). \tag{65}$$

The problem (65) can be addressed via a path-following procedure similar to Algorithm 2 where the following convex program is solved for κ-iteration:

$$\max_{\mathbf{V}, \boldsymbol{\rho}} \sum_{(i,j_\mathsf{D})\in\mathcal{S}_1} \frac{\zeta_{i,j_\mathsf{D}}}{2}\Big(\phi_{i,j_\mathsf{D}}^{(\kappa)}(\mathbf{V}_\mathsf{D}^E, 0_\mathsf{U}) - Q_{i,j_\mathsf{D}}(\mathbf{V}_\mathsf{D}^E, 0_\mathsf{U}, \boldsymbol{\rho}) + \phi_{i,j_\mathsf{D}}^{(\kappa)}(0_\mathsf{D}, \mathbf{V}_\mathsf{U})\Big) \quad \text{s.t.} \quad (39c), (40), (39d), (39e), (61d), (61e), \tag{66}$$

where $\phi_{i,j_\mathsf{D}}^{(\kappa)}(\mathbf{V}_\mathsf{D}^E, 0_\mathsf{U})$ ($\phi_{i,j_\mathsf{D}}^{(\kappa)}(0_\mathsf{D}, \mathbf{V}_\mathsf{U})$, resp.) is defined by (22) with both $\mathbf{V}_\mathsf{U}$ and $V_\mathsf{U}^{(\kappa)}$ (both $\mathbf{V}_\mathsf{D}$ and $V_\mathsf{D}^{(\kappa)}$, resp.) replaced by 0_U (0_D, resp.).

Problems (55), (58), (61), (64) and (66) involve $n = 2(N_1 d_1 ID + N_r d_2 IU) + 3$ scalar real decision variables and $m = ID + IU + 2I + 3$ quadratic constraints so its computational complexity is $O(n^2 m^{2.5} + m^{3.5})$.

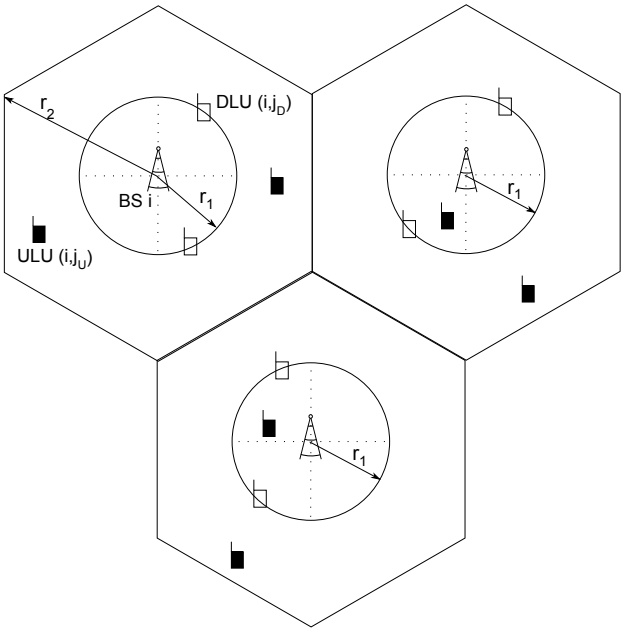

Fig. 2. A three-cell network with 3 DLUs and 3 ULUs. DLUs are randomly located on the circles with radius of r_1 centered at their serving BS. ULUs are uniformly distributed within the cell of their serving BS.

V. Numerical results

In this simulation study, we use the example network in Fig. 2 to study the total network throughput in the presence of SI. The HD system is also implemented as a base line for both time splitting mechanism and power splitting mechanism. DLUs are randomly located on the circles with radius of $r_1 = 20$ m centered at their serving BSs whereas ULUs are uniformly distributed within the cell of their serving BSs whose radius are $r_2 = 40$ m. There are two DLUs and two ULUs within each cell. We set the path loss exponent $\beta = 4$. For small-scale fading, we generate the channel matrices $H_{m,i,j_{\mathsf{D}}}$ from BS m to UE (i, j_{D}), matrices $H_{i,j_{\mathsf{D}},\ell_{\mathsf{U}}}$ from ULU (i, ℓ_{U}) to DLU (i, j_{D}), matrices $H_{m,\ell_{\mathsf{U}},i}$ from ULU (m, ℓ_{U}) to BS i and matrices $H^{\mathcal{B}}_{m,i}$ from BS m to BS i using the Rician fading model as follows:

$$H = \sqrt{\frac{K_R}{1+K_R}}H^{LOS} + \sqrt{\frac{1}{1+K_R}}H^{NLOS}, \tag{67}$$

where $K_R = 10$ dB is the Rician factor, H^{LOS} is the line-of-sight (LOS) deterministic component and each element of Rayleigh fading component H^{NLOS} is the circularly-symmetric complex Gaussian random variable $\mathcal{CN}(0,1)$. Here, we use the far-field uniform linear antenna array model [32] with

$$\begin{aligned} H^{LOS} = \; & [1, e^{j\theta_r}, e^{j2\theta_r}, \ldots, e^{j(N_r-1)\theta_r}] \\ & \times [1, e^{j\theta_t}, e^{j2\theta_t}, \ldots, e^{j(N_1-1)\theta_t}]^H, \end{aligned} \tag{68}$$

for $\theta_r = \frac{2\pi d \sin(\phi_r)}{\lambda}$, $\theta_t = \frac{2\pi d \sin(\phi_t)}{\lambda}$, where $d = \lambda/2$ is the antenna spacing, λ is the carrier wavelength and ϕ_r, ϕ_t is the angle-of-arrival, the angle-of-departure, respectively. In our simulations, ϕ_r and ϕ_t are randomly generated between 0 and 2π. Unless stated otherwise, the number of transmit antennas and the number of receive antennas at a BS are set as $N_1 = N_2 = 4$. The numbers of concurrent downlink data streams and the numbers of concurrent uplink data streams are equal and $d_1 = d_2 = N_r$. To arrive at the final figures, we run each simulation 100 times and average out the result. In all simulations, we set $P = 23$ dBW, $P_i = 16$ dBW $\forall i \in \mathcal{I}$, $P_{i,j_{\mathsf{U}}} = 10$ dBW $\forall (i, j_{\mathsf{U}}) \in \mathcal{S}_2$, $\forall i \in \mathcal{I}$,$\zeta = 0.5$, $\sigma_c^2 = -90$ dBW, $\sigma^2 = -90$ dBW, $r^{\min}_{i,j_{\mathsf{D}}} = r^{\mathsf{D}} = 1$ bps/Hz and $r^{\min}_i = r^{\mathsf{U}} = Ur^{\mathsf{D}}$ bps/Hz. We further assume that the required harvested energies of all DLUs are the same and $e^{\min}_{i,j_{\mathsf{D}}} = e^{\min}$, $\forall (i, j_{\mathsf{D}})$. Unless stated otherwise, we set $e^{\min} = -20$ dBm as in [7], [33]. According to the current state-of-the-art-electronic circuitry, the sensitivity level of a typical energy harvester is around -20 dBm (0.01mW) [34], which means that we can activate the EH circuitry with that much amount of received power. The SI level σ^2_{SI} is choosen within the range of $[-150, -90]$ dB [1] as in [14], [16], [26] where $\sigma^2_{SI} = -150$ dB represents the almost perfect SI cancellation.

A. Single cell network

Firstly, we consider the sum throughput maximization problem and the total harvested energy in the single cell networks. This will facilitate the analysis of the impact of SI to the network performance since there is no intercell interference. The network setting in Fig. 2 is used but only one cell is considered.

Fig. 3 illustrates the comparison of total network throughput between the power splitting mechanism and the time splitting mechanism in both FD and HD systems. Though FD provides a substantial improvement in comparison to HD in both power splitting mechanism (25.8%) and time splitting mechanism (26.1%) for $N_r = 2$ [2] at $\sigma^2_{SI} = -150$ dB. Note that we cannot expect a FD system to achieve twice the throughput of that is achieved by a HD system. This is because even when the SI cancellation is perfect, DLUs in FD are still vulnerable to the intracell interference from the ULUs of the same cell. Moreover, DLUs and ULUs in HD are served with more BS's antennas, resulting in a larger spatial diversity. Consequently, FD cannot double HD's throughput even with the almost perfect SI cancellation.

When we reduce the number of antennas at UEs from $N_r = 2$ to $N_r = 1$, the total network throughput of FD is significantly reduced by 42% for the time splitting mechanism and by 41% for the power splitting mechanism at $\sigma^2_{SI} = -150$ dB. Notably, since UEs in FD are exposed to more sources of interference than UEs in HD, reducing the number of antennas of UEs degrades the performance of FD more than the counterpart of HD. Consequently, the improvement of FD in comparison to HD reduces to 16% at $\sigma^2_{SI} = -150$ dB for both time splitting mechanism and power splitting mechanism.

Fig. 4 further illustrates how the total throughput is distributed into the downlink and uplink channels in the time splitting mechanism. The behaviour of the power splitting mechanism is similar and omitted here for brevity. With the

[1] At $\sigma^2_{SI} = -90$ dB, if a BS transmits at full power (i.e. 16 dBW), the SI power is 16 dB stronger than the background AWGN.

[2] N_r has been defined in the begining of section II as the number of antennas of UEs (DLUs and ULUs).

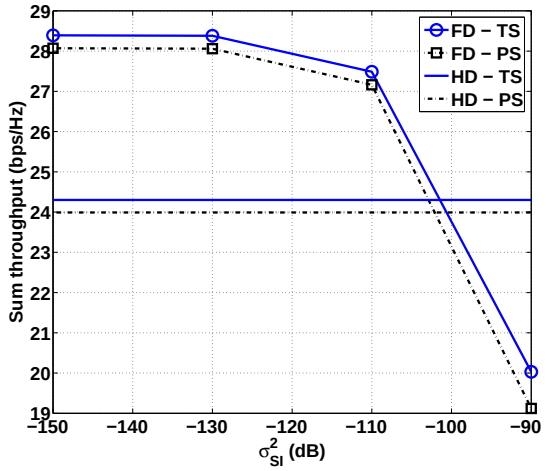

(a) $N_r = 1$

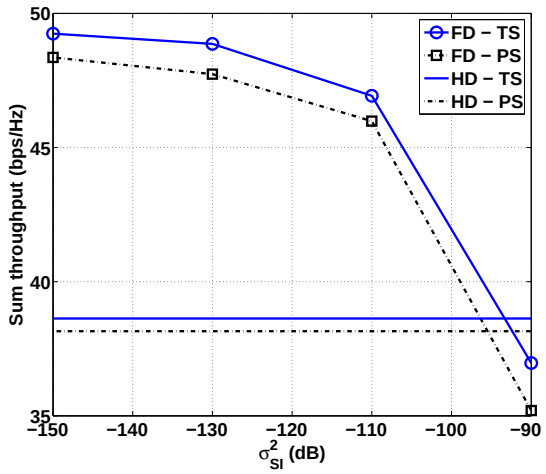

(b) $N_r = 2$

Fig. 3. Effect of SI on the sum throughput performance in the single-cell networks.

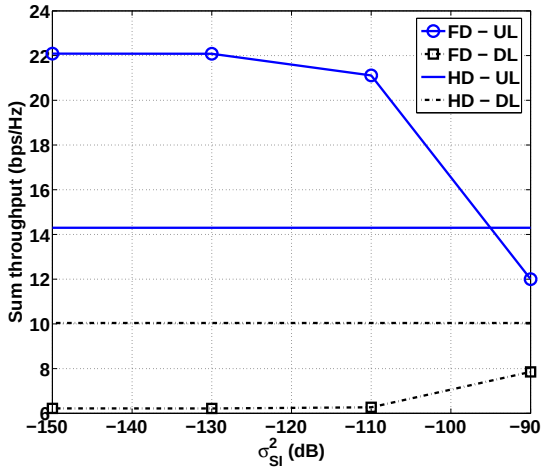

(a) $N_r = 1$

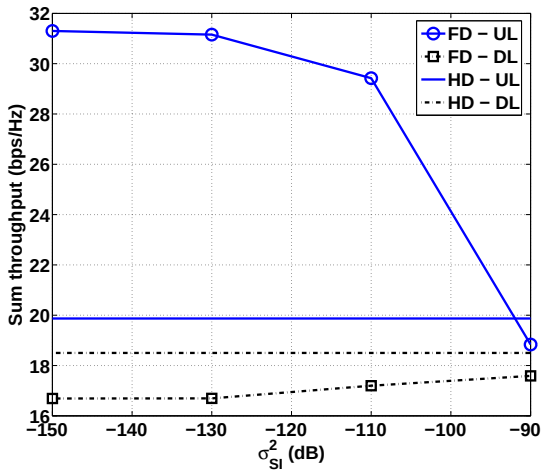

(b) $N_r = 2$

Fig. 4. Effect of SI on the UL/DL throughput performance in the single-cell networks.

increase of σ_{SI}^2, the UL throughput consistently decreases. Moreover, since the UL transmission becomes less efficient, ULUs reduce their transmission power to reduce the interference toward DLUs. Consequently, a slight increase in FD DL throughput is observed as σ_{SI}^2 increases. Another note is that since the distance between ULU-DLU in small cell can be quite small due to the random deployment of ULUs and DLUs, DLUs' throughput can be severely degraded by the interference from ULUs. In fact, the FD DL throughput is 60% less than the counterpart of HD at $N_r = 1, \sigma_{SI}^2 = -150$ dB. By implementing multiple antenna at UEs (i.e. $N_r = 2$), DLUs in FD can handle the interference better and the FD DL throughput at $\sigma_{SI}^2 = -150$ dB is only 10% less than the counterpart of HD.

To analyze the effect of energy harvesting constraint, we fix $N_r = 2, \sigma_{SI}^2 = -110$ dB and vary $e^{\min}$. Fig. 5 illustrates a consistent decreasing trend of all schemes as $e^{\min}$ increases. The time splitting scheme outperforms the power splitting scheme in the considered range of $e^{\min}$ for both FD and HD. A similar conclusion can be drawn from Fig. 3. By using two different precoder matrices $\mathbf{V}^I$ and $\mathbf{V}^E$ for data transmission and energy transferring, the time splitting scheme can exploit the spatial diversity better than the power splitting scheme which only uses one type of precoder matrix for both purposes. Thus, the time splitting scheme is more efficient than the power splitting scheme in term of performance.

The comparison of maximum harvested energy of time splitting scheme in both FD and HD systems is studied in Fig. 6. Interestingly, in case of $N_r = 1$, FD roughly harvests as much as HD. The reason of this is two folds. Firstly, it has been reported in [16], [26], [35] that FD not always harness performance gain over HD if the distance between ULUs and DLUs are not large enough. Since we consider small cell networks with randomly deployed ULUs and DLUs, the ULU-DLU distance can be very small, which creates significant interference to DLUs. Secondly, with $N_r = 1$, DLUs can not exploit the spatial diversity to mitigate the interference from ULUs. Consequently, ULUs must reduce its transmit power to ensure the QoS at the DLUs, which lowers the amount of harvested energy at DLUs. In contrast, the results show that

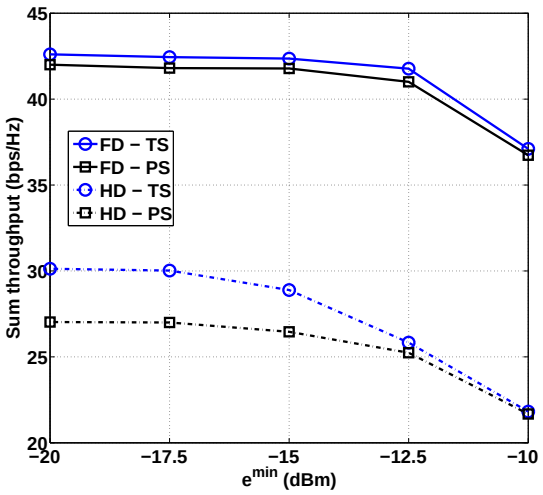

(a) $P_i = 30$ dBm

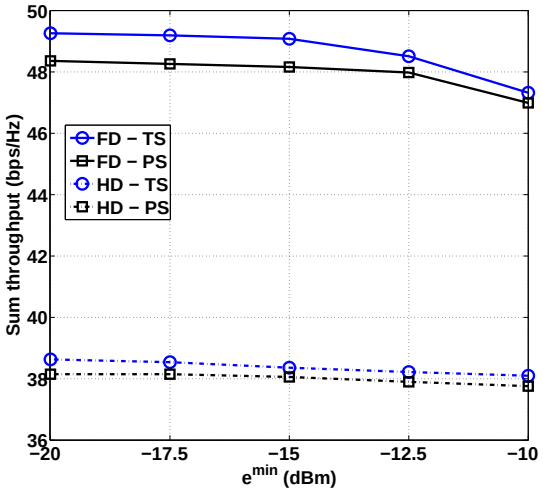

(b) $P_i = 46$ dBm

Fig. 5. Effect of energy harvesting constraints on the total harvested energy performance in the single-cell networks.

FD harvests more energy than HD given that $\sigma_{SI}^2 \leq -90$ dB for $N_r = 2$. All this implies that having multiple antennas at UEs is important to combat with extra interferences in FD.

B. Three-cell network

Now, we consider the sum throughput maximization problem and the total harvested energy in the three-cell networks as depicted in Fig. 2. In this scenario, DLUs and BSs are exposed to additional intercell interferences. According to Fig. 7, FD now only provides a marginal improvement regarding HD in both power splitting scheme (11.7%) and time splitting scheme (11.8%) for $N_r = 2, \sigma_{SI}^2 = -150$ dB. For $N_r = 1, \sigma_{SI}^2 = -150$ dB, the improvement is even lower with 4.1% in case of the power splitting scheme and 4.4% in case of time splitting scheme. Therefore, FD can give marginal gains compared to HD in the multi-cell networks with high level of interference.

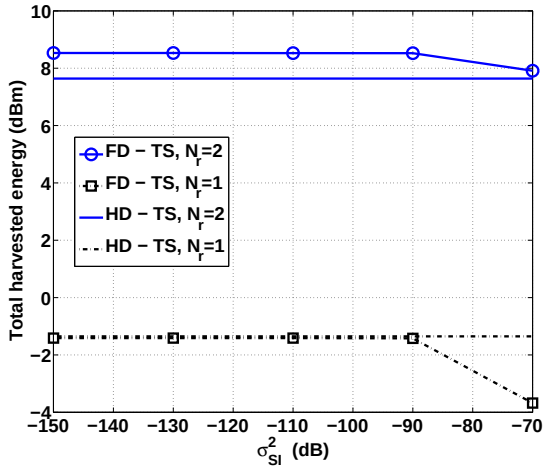

Fig. 6. Effect of SI on the total harvested energy performance in the single-cell networks.

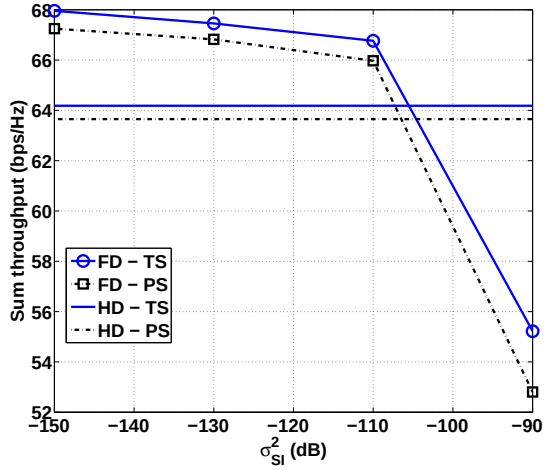

(a) $N_r = 1$

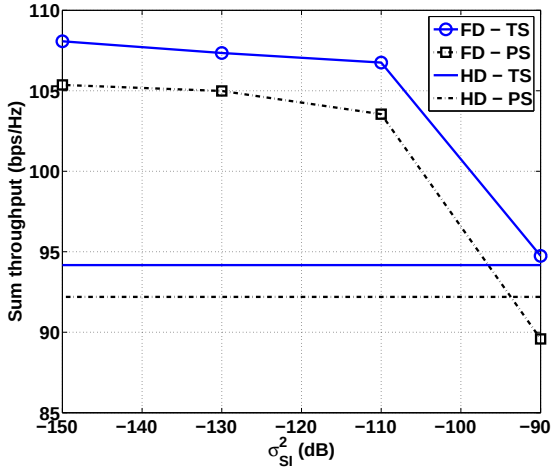

(b) $N_r = 2$

Fig. 7. Effect of SI on the sum throughput performance in the three-cell networks.

The effect of energy harvesting constraint to the network

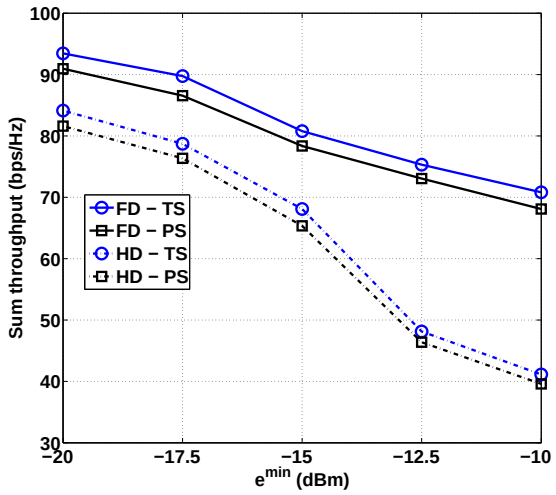

(a) $P_i = 30$ dBm

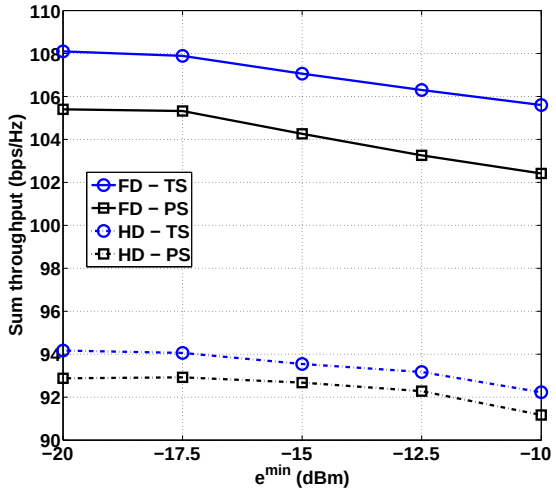

(b) $P_i = 46$ dBm

Fig. 8. Effect of energy harvesting constraints on the total harvested energy performance in the three-cell networks.

sum throughput is also investigated in Fig. 8 for the three-cell networks with $N_r = 2, \sigma_{SI}^2 = -110$ dB. As in Fig. 5, a consistent decreasing trend of all schemes is observed as $e^{\min}$ increases. Since DLUs can also harvest energy from the signals arriving from other BSs in multicell networks, the FD network throughput only decreases by about 3% for both harvesting scheme when $e^{\min}$ increases from -20 dBm to -10 dBm. The counterpart throughput decrease in single-cell scenarios was about 8%.

Fig. 9 also illustrates the comparison of total harvested energy per cell of the EH maximization problem in both FD and HD systems in three-cell network. For $N_r = 1$, FD even harvests lesser amount of energy than HD given $\sigma_{SI}^2 > -150$ dB due to the increasing level of interference when compared to a single-cell network. Similar to the single-cell network, FD outperforms HD for $\sigma_{SI}^2 \leq -90$ dB if more antennas are equipped at UEs (i.e. $N_r = 2$). This observation again emphasizes the importance of having multiple antenna at UEs

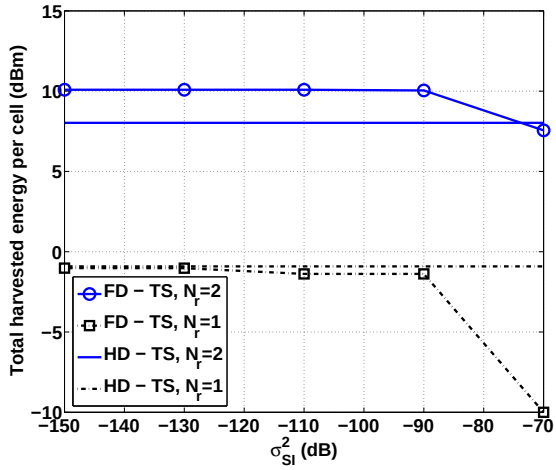

Fig. 9. Effect of SI on the total harvested energy performance in the three-cell networks.

in FD to mitigate interference. Another note is that given $N_r = 2$ the amount of energy harvested per cell in three-cell networks (i.e. 10.09 dBm at $\sigma_{SI}^2 = -150$ dB) is much higher than the harvested energy of single cell in Fig. 6 (i.e. 8.5 dBm at $\sigma_{SI}^2 = -150$ dB), thanks to the extra energy harvested from the intercell interference.

C. Convergence behaviour

Finally, the convergence behavior of the proposed Algorithm 1 is illustrated in Fig. 10. For brevity, we only present the case of the three-cell network at $\sigma_{SI}^2 = -110$ dB and $N_r = 2$. Fig. 10(a) plots the convergence of the objective functions of the sum throughput maximization problem for the time splitting scheme and the power splitting scheme, whereas Fig. 10(b) plots the convergence of the objective function of the EH maximization problem. As can be seen, the sum throughput maximization problem achieve 90% of its final optimal value within 40 iterations whereas the EH maximization problem needs 10 iterations. Table I shows the average number of iterations required to solve each program. Note that each iteration of the proposed algorithms invokes a convex subproblem to generate a new feasible point $(V_{\mathsf{D}}^{(\kappa+1)}, V_{\mathsf{U}}^{(\kappa+1)}, \alpha^{(\kappa+1)})$ that is better than the incumbent $(V_{\mathsf{D}}^{(\kappa)}, V_{\mathsf{U}}^{(\kappa)}, \alpha^{(\kappa)})$. Such a convex subproblem can be solved efficiently by the available convex solvers of polynomial complexity such as CVX [36]. To save the computational time, it is recommended to input the incumbent $(V_{\mathsf{D}}^{(\kappa)}, V_{\mathsf{U}}^{(\kappa)}, \alpha^{(\kappa)})$ as the initial point for the process of solving this subproblem. Also, the high dimensionality and the nonconvexity of the considered problems imply that checking the global optimality of the computed solution is both theoretically and practically prohibitive. Nevertheless, our recent results in [9] and [10] for the particular multi-input single output (MISO) case of the HD optimization problem (29) show that both Algorithm 1 and Algorithm 2 are capable of delivering the global optimal solutions.

VI. Conclusion

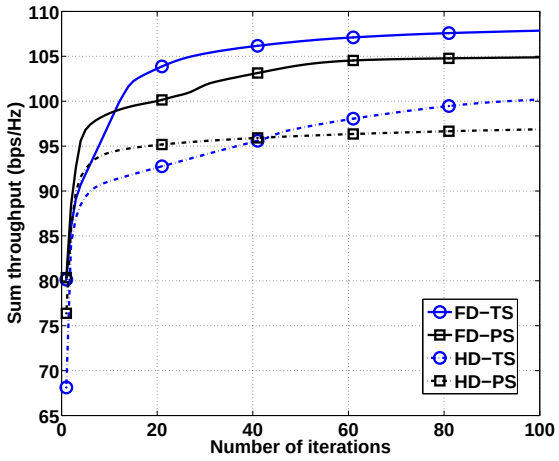

(a) Sum throughput maximization

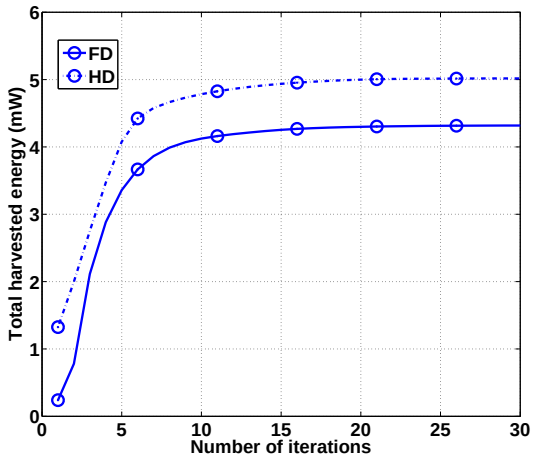

(b) EH maximization

Fig. 10. Convergence of the proposed algorithm for $\epsilon = 10^{-4}$.

TABLE I
THE AVERAGE NUMBER OF ITERATIONS REQUIRED BY THE PROPOSED ALGORITHMS

Programs	Throughput max., TS	Throughput max., PS	EH max.
FD	74	65.4	24.1
HD	67.5	50.6	20.2

We have proposed new optimal precoding designs for EH-enabled FD multicell MU-MIMO networks. Specifically, sum throughput maximization under throughput QoS constraints and EH constraints for energy-constrained devices under either TS or PS has been considered. The FD EH maximization problem under throughput QoS constraints in TS has also been addressed. Toward this end, we have developed new path-following algorithms for their solution, which require a convex quadratic program for each iteration and are guaranteed to monotonically converge at least to a local optimum. Finally, we have demonstrated the merits of our proposed algorithms through extensive simulations. Note that an interesting topic for further research is this area is robust precoder/beamformer design in the presence of channel estimation errors.

REFERENCES

[1] X. Lu, D. Niyato, P. Wang, and D. I. Kim, "Wireless charger networking for mobile devices: fundamentals, standards, and applications," *IEEE Wireless Commun. Mag.*, vol. 22, no. 2, pp. 126–135, Apr. 2015.

[2] X. Lu, P. Wang, D. Niyato, D. I. Kim, and Z. Han, "Wireless charging technologies: Fundamentals, standards, and network applications," *IEEE Commun. Surveys Tutorials*, vol. 18, no. 2, pp. 1413–1452, Second Quarter 2016.

[3] S. Buzzi, C. L. I, T. E. Klein, H. V. Poor, C. Yang, and A. Zappone, "A survey of energy-efficient techniques for 5G networks and challenges ahead," *IEEE J. Sel. Areas Commun.*, vol. 34, no. 4, pp. 697–709, Apr. 2016.

[4] J. G. Andrews, S. Buzzi, W. Choi, S. V. Hanly, A. Lozano, A. C. K. Soong, and J. C. Zhang, "What will 5G be?" *IEEE J. Sel. Areas Commun.*, vol. 32, no. 6, pp. 1065–1082, Jun. 2014.

[5] Z. Ding, C. Zhong, D. W. K. Ng, M. Peng, H. A. Suraweera, R. Schober, and H. V. Poor, "Application of smart antenna technologies in simultaneous wireless information and power transfer," *IEEE Commun. Mag.*, vol. 53, no. 4, pp. 86–93, Apr. 2015.

[6] S. Timotheou, I. Krikidis, G. Zheng, and B. Ottersten, "Beamforming for MISO interference channels with QoS and RF energy transfer," *IEEE Trans. Wireless Commun.*, vol. 13, no. 5, pp. 2646–2658, May 2014.

[7] Q. Shi, W. Xu, T. H. Chang, Y. Wang, and E. Song, "Joint beamforming and power splitting for MISO interference channel with SWIPT: An SOCP relaxation and decentralized algorithm," *IEEE Trans. Signal Process.*, vol. 62, no. 23, pp. 6194–6208, Dec. 2014.

[8] A. A. Nasir, D. T. Ngo, H. D. Tuan, and S. Durrani, "Iterative optimization for max-min SINR in dense small-cell multiuser MISO SWIPT system," in *Proc. IEEE Global Conf. on Signal Processing (GlobalSIP)*, 2015, pp. 1392–1396.

[9] A. A. Nasir, H. D. Tuan, D. T. Ngo, S. Durrani, and D. I. Kim, "Path-following algorithms for beamforming and signal splitting in RF energy harvesting networks," *IEEE Commun. Letters*, vol. 20, no. 8, pp. 1687–1690, Aug 2016.

[10] A. A. Nasir, H. D. Tuan, D. T. Ngo, T. Q. Duong, and H. V. Poor, "Beamforming design for wireless information and power transfer systems: Receive power-splitting versus transmit time-switching," *IEEE Trans. Commun.*, vol. 65, no. 2, pp. 876–889, Feb. 2017.

[11] J. Park and B. Clerckx, "Joint wireless information and energy transfer in a K-user MIMO interference channel," *IEEE Trans. Wireless Commun.*, vol. 13, no. 10, pp. 5781–5796, Oct. 2014.

[12] ——, "Joint wireless information and energy transfer with reduced feedback in MIMO interference channels," *IEEE J. Sel. Areas Commun.*, vol. 33, no. 8, pp. 1563–1577, Aug. 2015.

[13] R. Zhang and C. K. Ho, "MIMO broadcasting for simultaneous wireless information and power transfer," *IEEE Trans. Wireless Commun.*, vol. 12, no. 5, pp. 1989–2001, May 2013.

[14] D. Nguyen, L.-N. Tran, P. Pirinen, and M. Latva-aho, "Precoding for full duplex multiuser MIMO systems: Spectral and energy efficiency maximization," *IEEE Trans. Signal Process.*, vol. 61, no. 16, pp. 4038–4050, Aug. 2013.

[15] Z. Zong, H. Feng, F. R. Yu, N. Zhao, T. Yang, and B. Hu, "Optimal transceiver design for SWIPT in K-user MIMO interference channels," *IEEE Trans. Wireless Commun.*, vol. 15, no. 1, pp. 430–445, Jan. 2016.

[16] H. H. M. Tam, H. D. Tuan, and D. T. Ngo, "Successive convex quadratic programming for quality-of-service management in full-duplex MU-MIMO multicell networks," *IEEE Trans. Commun.*, vol. 64, no. 6, pp. 2340–2353, Jun. 2016.

[17] E. Everett, A. Sahai, and A. Sabharwal, "Passive self-interference suppression for full-duplex infrastructure nodes," *IEEE Trans. Wireless Commun.*, vol. 13, no. 2, pp. 680–694, Feb. 2014.

[18] M. Duarte, A. Sabharwal, V. Aggarwal, R. Jana, K. Ramakrishnan, C. Rice, and N. Shankaranarayanan, "Design and characterization of a full-duplex multiantenna system for WiFi networks," *IEEE Trans. Veh. Technol.*, vol. 63, no. 3, pp. 1160–1177, Mar. 2014.

[19] L. Anttila et al, "Modeling and efficient cancelation of nonlinear self-interference in MIMO full-duplex transceivers," in *Proc. IEEE Global Conf. on Communication (Globecom)*, Dec. 2014, pp. 777–783.

[20] M. Heino et al, "Recent advances in antenna design and interference cancelllation algorithms for in-band full duplex relays," *IEEE Commun. Mag.*, vol. 53, no. 5, pp. 91–101, May 2015.

[21] M. Duarte, C. Dick, and A. Sabharwal, "Experiment-driven characterization of full-duplex wireless systems," *IEEE Trans. Wireless Commun.*, vol. 11, no. 12, pp. 4296–4307, Dec. 2012.

[22] Y.-S. Choi and H. Shirani-Mehr, "Simultaneous transmission and reception: Algorithm, design and system level performance," *IEEE Trans. Wireless Commun.*, vol. 12, no. 12, pp. 5992–6010, Dec. 2013.
[23] A. Sabharwal et al, "In-band full-duplex wireless: challenges and opportunities," *IEEE J. Select. Areas. Commun.*, vol. 32, no. 9, pp. 1637–1652, Sep 2014.
[24] "System scenarios and technical requirements for full-duplex concept," *DUPLO project, Deliverable D1.1*. [Online]. Available: athttp://www.fp7-duplo.eu/index.php/deliverables.
[25] S. Huberman and T. Le-Ngoc, "MIMO full-duplex precoding: A joint beamforming and self-interference cancellation structure," *IEEE Trans. Wireless Commun.*, vol. 14, no. 4, pp. 2205–2217, Apr. 2015.
[26] D. Nguyen, L.-N. Tran, P. Pirinen, and M. Latva-aho, "On the spectral efficiency of full-duplex small cell wireless systems," *IEEE Trans. Wireless Commun.*, vol. 13, no. 9, pp. 4896–4910, Sep. 2014.
[27] H. H. Kha, H. D. Tuan, and H. H. Nguyen, "Fast global optimal power allocation in wireless networks by local d.c. programming," *IEEE Trans. Wireless Commun.*, vol. 11, no. 2, pp. 510–515, Feb. 2012.
[28] H. Tuy, *Convex Analysis and Global Optimization*. Kluwer Academic, 1998.
[29] B. Day, A. R. Margetts, D. Bliss, and P. Schniter, "Full-duplex bidirectional MIMO: Achievable rates under limited dynamic range," *IEEE Trans. Signal Process.*, vol. 60, no. 7, pp. 3702–3713, Jul. 2012.
[30] D. Tse and P. Viswanath, *Fundamentals of Wireless Communication*. New York, NY, USA: Cambridge University Press, 2005.
[31] D. Katselis, E. Kofidis, and S. Theodoridis, "On training optimization for estimation of correlated MIMO channels in the presence of multiuser interference," *IEEE Trans. Signal Process.*, vol. 56, no. 10, pp. 4892–4904, Oct. 2008.
[32] Y. S. Cho, J. Kim, W. Y. Yang, and C. G. Kang, *MIMO- OFDM Wireless Commun. with MATLAB*. John Wiley & Sons, Ltd, 2010.
[33] Q. Shi, W. Xu, J. Wu, E. Song, and Y. Wang, "Secure beamforming for mimo broadcasting with wireless information and power transfer," *IEEE Trans. Wireless Commun.*, vol. 14, no. 5, pp. 2841–2853, May 2015.
[34] ——, "Secure beamforming for mimo broadcasting with wireless information and power transfer," *IEEE Trans. Wireless Commun.*, vol. 14, no. 5, pp. 2841–2853, May 2015.
[35] M. Mohammadi, H. A. Suraweera, Y. Cao, I. Krikidis, and C. Tellambura, "Full-duplex radio for uplink/downlink wireless access with spatially random nodes," *IEEE Trans. Commun.*, vol. 63, no. 12, pp. 5250–5266, Dec. 2015.
[36] M. Grant and S. Boyd, "CVX: Matlab software for disciplined convex programming, version 2.1," http://cvxr.com/cvx, Mar. 2014.

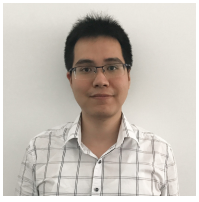

Ho Huu Minh Tam was born in Ho Chi Minh City, Vietnam. He received the B.S. degree in electrical engineering and telecommunications from the Ho Chi Minh City University of Technology in 2012, and he is currently pursuing the Ph.D. degree with the University of Technology Sydney, NSW, Australia, under the supervision of Prof. H. D. Tuan. His research interest is in optimization techniques in signal processing for wireless communications.

Hoang Duong Tuan received the Diploma (Hons.) and Ph.D. degrees in applied mathematics from Odessa State University, Ukraine, in 1987 and 1991, respectively. He spent nine academic years in Japan as an Assistant Professor in the Department of Electronic-Mechanical Engineering, Nagoya University, from 1994 to 1999, and then as an Associate Professor in the Department of Electrical and Computer Engineering, Toyota Technological Institute, Nagoya, from 1999 to 2003. He was a Professor with the School of Electrical Engineering and Telecommunications, University of New South Wales, from 2003 to 2011. He is currently a Professor with the Faculty of Engineering and Information Technology, University of Technology Sydney. He has been involved in research with the areas of optimization, control, signal processing, wireless communication, and biomedical engineering for more than 20 years.

Ali Arshad Nasir (S'09-M'13) is an Assistant Professor in the Department of Electrical Engineering, King Fahd University of Petroleum and Minerals (KFUPM), Dhahran, KSA. Previously, he held the position of Assistant Professor in the School of Electrical Engineering and Computer Science (SEECS) at National University of Sciences & Technology (NUST), Paksitan, from 2015-2016. He received his Ph.D. in telecommunications engineering from the Australian National University (ANU), Australia in 2013 and worked there as a Research Fellow from 2012-2015. His research interests are in the area of signal processing in wireless communication systems. He is an Associate Editor for IEEE Canadian Journal of Electrical and Computer Engineering.

Trung Q. Duong (S'05, M'12, SM'13) received his Ph.D. degree in Telecommunications Systems from Blekinge Institute of Technology (BTH), Sweden in 2012. Since 2013, he has joined Queen's University Belfast, UK as a Lecturer (Assistant Professor). His current research interests include small-cell networks, physical layer security, energy-harvesting communications, cognitive relay networks. He is the author or co-author of 240 technical papers published in scientific journals (125 articles) and presented at international conferences (115 papers).

Dr. Duong currently serves as an Editor for the IEEE TRANSACTIONS ON WIRELESS COMMUNICATIONS, IEEE TRANSACTIONS ON COMMUNICATIONS, IET COMMUNICATIONS, and a Senior Editor for IEEE COMMUNICATIONS LETTERS. He was awarded the Best Paper Award at the IEEE Vehicular Technology Conference (VTC-Spring) in 2013, IEEE International Conference on Communications (ICC) 2014, and IEEE Global Communications Conference (GLOBECOM) 2016. He is the recipient of prestigious Royal Academy of Engineering Research Fellowship (2016-2021).

H. Vincent Poor (S72, M77, SM82, F87) received the Ph.D. degree in EECS from Princeton University in 1977. From 1977 until 1990, he was on the faculty of the University of Illinois at Urbana-Champaign. Since 1990 he has been on the faculty at Princeton, where he is currently the Michael Henry Strater University Professor of Electrical Engineering. During 2006 to 2016, he served as Dean of Princetons School of Engineering and Applied Science. His research interests are in the areas of information theory, statistical signal processing and stochastic analysis, and their applications in wireless networks and related fields such as smart grid and social networks. Among his publications in these areas is the book *Mechanisms and Games for Dynamic Spectrum Allocation* (Cambridge University Press, 2014).

Dr. Poor is a member of the National Academy of Engineering, the National Academy of Sciences, and is a foreign member of the Royal Society. He is also a fellow of the American Academy of Arts and Sciences, the National Academy of Inventors, and other national and international academies. He received the Marconi and Armstrong Awards of the IEEE Communications Society in 2007 and 2009, respectively. Recent recognition of his work includes the 2016 John Fritz Medal, the 2017 IEEE Alexander Graham Bell Medal, Honorary Professorships at Peking University and Tsinghua University, both conferred in 2016, and a D.Sc. *honoris causa* from Syracuse University awarded in 2017.